MULTIPLE SYMBOL DECODING OF DIFFERENTIAL SPACE-TIME CODES

A Thesis

by

ROHIT SINGHAL

Submitted to the Office of Graduate Studies of
Texas A&M University
in partial fulfillment of the requirements for the degree of

MASTER OF SCIENCE

December 2003

Major Subject: Electrical Engineering

MULTIPLE SYMBOL DECODING OF

DIFFERENTIAL SPACE-TIME CODES

A Thesis

by

ROHIT SINGHAL

Submitted to Texas A&M University
in partial fulfillment of the requirements
for the degree of

MASTER OF SCIENCE

Approved as to style and content by:

Xiaodong Wang (Co-Chair of Committee)	Costas N. Georghiades (Co-Chair of Committee)
A.L.N. Reddy (Member)	Rabi Mahapatra (Member)
Chanan Singh (Head of Department)	

December 2003

Major Subject: Electrical Engineering

ABSTRACT

Multiple Symbol Decoding of

Differential Space-Time Codes. (December 2003)

Rohit Singhal, B.Tech., Indian Institute of Technology Kharagpur, INDIA

Co–Chairs of Advisory Committee: Dr. Xiaodong Wang
Dr. Costas N. Georghiades

Multiple-symbol detection of space-time differential codes (MS-STDC) decodes N consecutive space-time symbols using maximum likelihood (ML) sequence detection to gain in performance over the conventional differential detection scheme. However its computational complexity is exponential in N. A fast algorithm for implementing the MD-STDC in block-fading channels with complexity $\mathcal{O}(N^4)$ is developed. Its performance in both block-fading and symbol-by-symbol fading channels is demonstrated through simulations.

Set partitioning in hierarchical trees (SPIHT) coupled with rate compatible punctured convolution code (RCPC) and cyclic redundancy check (CRC) is employed as a generalized multiple description source coder with robustness to channel errors. We propose a serial concatenation of the above with a differential space-time code (STDC) and invoke an iterative *joint source channel decoding* procedure for decoding differentially space-time coded multiple descriptions. Experiments show a gain of up to 5 dB in PSNR with four iterations for image transmission in the absence of channel state information (CSI) at the receiver. A serial concatenation of SPIHT + RCPC/CRC is also considered with space-time codes (STC) instead of STDC. Experiments show a gain of up to 7 dB with four iterations in the absence of CSI.

To My Parents and Richa

ACKNOWLEDGMENTS

I gratefully acknowledge the support, guidance and encouragement that I received from my advisor, Dr. Xiaodong Wang, throughout the course of my studies. He gave me the confidence and the tools necessary to complete this work. I would also like to thank Dr. Costas N. Georghiades for his encouragement and a never tiring helping hand.

I would like to thank my committee members, Dr. Rabi Mahapatra and Dr. A.L.N. Reddy, for their advice and encouragement. I thank Dr. Zixiang Xiong for his important contributions to my research. I am grateful to Dr. Deepa Kundur and Dr. Ricardo Bettati for their support. They were kind enough to act as substitutes at my thesis defense on a very short notice.

This work benefited greatly from the interaction with all the members of the Wireless Communications Laboratory at Texas A&M University. In particular, I want to thank Mr. Vivek Gulati, Mr. Angelos Liveris, Mr. Hari Sankar, Mr. Nitin A. Nangare and Mr. Deepak Kumar, for their valuable contributions.

I would also like to acknowledge Veera, Waqar, Dali, Bhos, Deba, Gilra, Percy, Bhoju, Pankaj and Gullu for the good time that I had with them at Texas A&M University. Their company never let me feel away from home.

Finally, I thank my parents, Richa, Ravi, Michael and Tiwary for their love and support. I thank them for giving me the constant love, encouragement, inspiration and motivation without which this research would not have been possible.

TABLE OF CONTENTS

LIST OF FIGURES

FIGURE Page

CHAPTER I

INTRODUCTION

A. Multi-Symbol Detection of Differential Space-Time Codes

Space-time coding (STC) can provide significant capacity gains in wireless channels by integrating the techniques of multiple antenna spatial processing and channel coding [1]. Recently in [2, 3] space-time *differential* coding (STDC) schemes have been developed. The advantage of the differential scheme over STC is, that it does not require the information about the state of the channel at the receiver.

In the context of DPSK, a multiple-symbol differential detection (MSDD) scheme for additive white Gaussian noise (AWGN) channels was developed by Divsalar et al [4]. An improvement in performance is observed on increasing the detection window size, and it asymptotically reaches the performance of coherent detection. Even in flat-fading channels the MSDD shows impressive performance gains over the conventional single symbol detection scheme [5]. The MSDD however, has a computational complexity *exponential* in the block size N. In [6] a fast MSDD algorithm with a complexity $\mathcal{O}(N \log N)$ was developed.

Similarly, the performance of STDC can be significantly enhanced by using multiple-symbol detection as shown in [7]. Like MSDD, the complexity of the maximum likelihood (ML) MS-STDC detection is exponential in N. We try to develop a fast implementation which becomes necessary considering the huge improvements in performance MS-STDC can produce. The Fast algorithm is discussed in chapter II. The results are discussed in chapter V

The journal model is *IEEE Transactions on Automatic Control.*

B. Space-Time Coded Multiple Descriptions of Images

A maximum *a posteriori* (MAP) decoding algorithm for STDC developed by Nguyen and Ingram [8] showed that it is a recursive code and has a trellis structure . Therefore, it can also be decoded using the Viterbi or the BCJR algorithm [9]. Nguyen et al developed an efficient soft-in-soft-out (SISO) receiver for STDC which does not require the channel state information (CSI). They show through simulations that an iterative receiver for the serial concatenation (SC) of a STDC with a convolution code as the outer code produces better performance with each iteration.

Multiple description (MD) source coding is a technique that generates multiple correlated descriptions of a source. Any one of these descriptions can be used to reproduce the original source with certain fidelity. When more than one descriptions are available to the decoder, they can be synergistically combined to enhance the quality [10]. From a source coding viewpoint, MDs can be generated via MD quantization [11], MD correlating transforms [12], or MD coding with frames [13]. MD coding can also be viewed as a means of joint source-channel coding (JSCC). Under this context, the MDs can be easily generated with embedded coding and unequal error protection (UEP) [14, 15].

We consider transporting MDs over wireless $fading$ channels rather than the on-off channels considered in most earlier works. The idea is to treat MD coding as JSCC and use channel coding techniques developed for SC coding systems to improve the performance of the receiver with successive iterations [16, 17]. Iterative decoding was used in [18] to decode MDs transmitted over an AWGN channel. Results obtained on using a Gaussian source and two MD scalar quantizers [11] indicate that the efficacy of iterative decoding depends on the amount of correlation in the two descriptions.

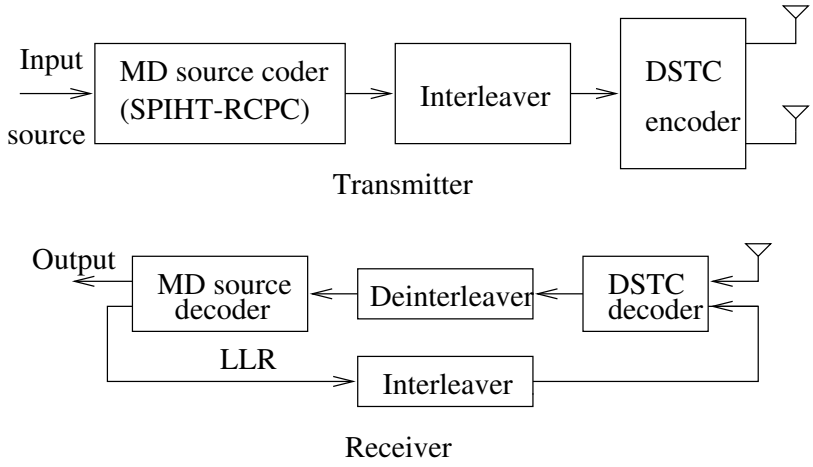

Fig. 1. The proposed serial concatenation of MD coding and STDC.

We propose to use SPIHT [1] + RCPC/CRC [2] [19, 20] as a generalized JSCC. We use this and an STDC as the two constituent codes to form a SC coding system. Our proposed receiver consists of a MAP differential space-time decoder [8], an MD source decoder, an interleaver and a deinterleaver. There are several ways to interpret the scheme in Fig. 1. We provide here only a motivating one. According to [21], STC or, for that matter, STDC asymptotically converts a fading channel into a Gaussian channel, for which the initial scheme [18] for iterative decoding of MDs was designed.

In [22] a SISO decoding algorithm for decoding STC has been developed based on the expectation-maximization (EM) algorithm [23]. Simulations show improvement in performance with successive iterations for coded Alamouti STC. We propose to modify the system described in the fig. 1 by replacing the STDC with the STC. The receiver end is updated by changing the STDC decoder with a modification of the receiver developed in [22]. The SC systems and the simulation results are discussed in chapters III, IV, and V.

[1] Set Partitioning in Hierarchical Trees.

[2] Rate Compatible Punctured Convolution Code with Cyclic Redundancy Check

CHAPTER II

A FAST ALGORITHM FOR MULTIPLE-SYMBOL DETECTION OF DIFFERENTIAL SPACE-TIME CODES

This chapter begins with the description of the STDC system in section A. As discussed in the chapter I, a multi-symbol decoding of differential space-time codes (MS-STDC), discussed in the section B, provides gain in performance over the conventional one-symbol decoding schemes. This improvement, however, comes at a prohibitive increase in complexity. A fast and exact implementation of the ML receiver, which becomes necessary, is discussed in C. The results are discussed in chapter V

A. Space-Time Differential Coding

STDC was first developed in [2, 3]. It is modified as described below for our system. Consider a communication system with two transmit antennas and one receive antenna. Let the M-ary PSK (M-PSK) symbols at time $2i$ and $2i+1$ be

$$\begin{aligned} a_{2i} &\in \mathcal{A} \triangleq \left\{ \frac{1}{\sqrt{2}} e^{j\frac{2\pi k}{M}},\ k = 0, 1, \cdots, M-1 \right\}. \\ a_{2i+1} &= \pm a_{2i}. \end{aligned} \tag{2.1}$$

Define the following matrices:

$$\underline{A}_0 \triangleq \begin{bmatrix} a_0 & a_1 \\ -a_1^* & a_0^* \end{bmatrix},$$

$$\underline{A}_i \triangleq \begin{bmatrix} a_{2i} & a_{2i+1} \\ -a_{2i+1}^* & a_{2i}^* \end{bmatrix}, \text{ for } i \geq 1, \tag{2.2}$$

$$\underline{G}_i \triangleq \underline{A}_i \underline{A}_0^H. \tag{2.3}$$

It is easy to see that $\underline{A}_i$ and $\underline{G}_i$ are both orthogonal matrices, i.e., $\underline{A}_i\underline{A}_i^H = \underline{A}_i^H\underline{A}_i = \underline{G}_i\underline{G}_i^H = \underline{G}_i^H\underline{G}_i = \boldsymbol{I}_2$. Hence, given $\underline{G}_i$, $\underline{A}_i$ can be obtained by

$$\underline{A}_i = \underline{G}_i\underline{A}_0. \tag{2.4}$$

Also, $\underline{G}_i$ is always an element of a finite set $\mathcal{G}$.

$$\underline{G}_i \in \mathcal{G} \triangleq \left\{ \begin{bmatrix} g & 0 \\ 0 & g^* \end{bmatrix}, \begin{bmatrix} 0 & g \\ -g^* & 0 \end{bmatrix} \right\}. \tag{2.5}$$

where, $\frac{g}{\sqrt{2}} \in \mathcal{A}$. For example, if $\mathcal{A}$ is a QPSK signal constellation, then,

$$\underline{G}_i \in \mathcal{G} \triangleq \left\{ \pm \begin{bmatrix} 1 & 0 \\ 0 & 1 \end{bmatrix}, \pm \begin{bmatrix} j & 0 \\ 0 & -j \end{bmatrix}, \pm \begin{bmatrix} 0 & 1 \\ -1 & 0 \end{bmatrix}, \pm \begin{bmatrix} 0 & j \\ j & 0 \end{bmatrix} \right\}. \tag{2.6}$$

The space-time differential block code is recursively defined as follows:

$$\begin{aligned} \underline{X}_0 &= \underline{A}_0, \\ \underline{X}_i &= \underline{G}_i\underline{X}_{i-1}, \quad i > 0. \end{aligned} \tag{2.7}$$

By a simple induction, it is easy to show that the matrix $\underline{X}_i$ has the following form

$$\underline{X}_i \triangleq \begin{bmatrix} x_{2i} & x_{2i+1} \\ -x_{2i+1}^* & x_{2i}^* \end{bmatrix}, \tag{2.8}$$

where $x_{2i}, x_{2i+1} \in \mathcal{A}$ and $\|x_{2i}\|^2 + \|x_{2i+1}\|^2 = 1$. Hence $\underline{X}_i$ is also an orthogonal matrix, and by (2.7), we have

$$\underline{X}_i\underline{X}_{i-1}^H = \underline{G}_i. \tag{2.9}$$

At time slot $2i$, the symbols on the first row of $\underline{X}_i$ in (2.8), x_{2i} and x_{2i+1} are

transmitted simultaneously from antenna 1 and antenna 2, respectively. At time slot $2i+1$, the symbols on the second row of $\underline{X}_i$, $-x_{2i+1}^*$ and x_{2i}^* are transmitted simultaneously from the two antennas. We consider the case where the channel is block-fading, i.e., it remains static over a block of symbols and it varies from block to block. Let α_1 and α_2 be the complex fading gains between the two transmit antennas and the receive antenna, respectively. The received signals at time slots $2i$ and $2i+1$ are then given respectively by

$$y_{2i} = \alpha_1 x_{2i} + \alpha_2 x_{2i+1} + v_{2i}, \tag{2.10}$$

$$y_{2i+1} = -\alpha_1 x_{2i+1}^* + \alpha_2 x_{2i}^* + v_{2i+1}, \tag{2.11}$$

where v_{2i} and v_{2i+1} are independent zero-mean symmetric complex Gaussian noise samples with variance σ^2 . Note that from (2.10) and (2.11), in the absence of noise, we can write the following:

$$\underbrace{\begin{bmatrix} y_{2i}^* & y_{2i+1}^* \\ y_{2i+1} & -y_{2i} \end{bmatrix}}_{\underline{Y}_i} = \underbrace{\begin{bmatrix} \alpha_1^* & \alpha_2^* \\ \alpha_2 & -\alpha_1 \end{bmatrix}}_{\underline{H}} \underbrace{\begin{bmatrix} x_{2i}^* & -x_{2i+1} \\ x_{2i+1}^* & x_{2i} \end{bmatrix}}_{\underline{X}_i^H}. \tag{2.12}$$

Since

$$\underline{H}^H \underline{H} = \left(|\alpha_1|^2 + |\alpha_2|^2\right) \boldsymbol{I}_2, \tag{2.13}$$

then using (2.9) and (2.12) , we have

$$\begin{aligned} \underline{Y}_i^H \underline{Y}_{i-1} &= \left(|\alpha_1|^2 + |\alpha_2|^2\right) \underline{X}_i \underline{X}_{i-1}^H, \\ &= \left(|\alpha_1|^2 + |\alpha_2|^2\right) \underline{G}_i. \end{aligned} \tag{2.14}$$

Based on the above discussion, we arrive at the following differential space-time de-

coding algorithm.

Algorithm 1 (Differential Space-Time Decoding) *Given the initial information symbol matrix* $\underline{A}_0$*, let* $\hat{\underline{A}}_0 = \underline{A}_0$*. Form* $\underline{Y}_0$ *according to (2.12) using* y_0 *and* y_1*. For* $i = 1, 2, \cdots$,

- *Form the matrix* $\underline{Y}_i$ *according to (2.12) using* y_{2i} *and* y_{2i+1}*.*
- *Obtain an estimate* $\hat{\underline{G}}_i$ *of* $\underline{G}_i$ *which is closest to* $\underline{Y}_i^H \underline{Y}_{i-1}$*.*
- *Perform the following mapping* $\hat{\underline{A}}_i = \hat{\underline{G}}_i \hat{\underline{A}}_0$*.*

B. Multiple-Symbol STDC Decoding

We now rewrite (2.10) and (2.11) as follows,

$$\underbrace{\begin{bmatrix} y_{2i} \\ y_{2i+1} \end{bmatrix}}_{\underline{y}_i} = \underbrace{\begin{bmatrix} x_{2i} & x_{2i+1} \\ -x_{2i+1}^* & x_{2i}^* \end{bmatrix}}_{\underline{X}_i} \underbrace{\begin{bmatrix} \alpha_1 \\ \alpha_2 \end{bmatrix}}_{\boldsymbol{\alpha}} + \underbrace{\begin{bmatrix} v_{2i} \\ v_{2i+1} \end{bmatrix}}_{\boldsymbol{v}_i}. \tag{2.15}$$

Denote

$$\boldsymbol{y}_n \triangleq \begin{bmatrix} \underline{y}_n \\ \underline{y}_{n+1} \\ \vdots \\ \underline{y}_{n+N} \end{bmatrix} \quad \text{and} \quad \boldsymbol{X}_n \triangleq \begin{bmatrix} \underline{X}_n \\ \underline{X}_{n+1} \\ \vdots \\ \underline{X}_{n+N} \end{bmatrix}. \tag{2.16}$$

At the receiver, the pdf of the received signal vector $\boldsymbol{y}_n$ given $\boldsymbol{X}_n$ and $\boldsymbol{\alpha}$, is

$$\mathrm{p}(\boldsymbol{y}_n | \boldsymbol{X}_n, \boldsymbol{\alpha}) = \frac{1}{(\pi\sigma^2)^{2N}} \quad \exp\left(\frac{-\|\boldsymbol{y}_n - \boldsymbol{X}_n \boldsymbol{\alpha}\|^2}{\sigma^2} \right). \tag{2.17}$$

Now

$$\begin{aligned}\|\boldsymbol{y}_n - \boldsymbol{X}_n\boldsymbol{\alpha}\|^2 &= \sum_{i=n}^{n+N}\left(|y_{2i} - x_{2i}\alpha_1 - x_{2i+1}\alpha_2|^2 + |y_{2i+1} - x_{2i}^*\alpha_2 + x_{2i+1}^*\alpha_1|^2\right)\\ &= \sum_{i=n}^{n+N}\left(|y_{2i}|^2 + |y_{2i+1}|^2 + |\alpha_1|^2 + |\alpha_2|^2\right)\\ &\quad -2\Re\left(\alpha_1\sum_{i=n}^{n+N}(y_{2i}^*x_{2i} - y_{2i+1}^*x_{2i+1}^*)\right)\\ &\quad -2\Re\left(\alpha_2\sum_{i=n}^{n+N}(y_{2i}^*x_{2i+1} + y_{2i+1}^*x_{2i}^*)\right).\end{aligned} \tag{2.18}$$

For simplicity, denote

$$\eta_1 = \sum_{i=n}^{n+N}\left(y_{2i}^*x_{2i} - y_{2i+1}^*x_{2i+1}^*\right), \tag{2.19}$$

$$\eta_2 = \sum_{i=n}^{n+N}\left(y_{2i}^*x_{2i+1} + y_{2i+1}^*x_{2i}^*\right), \tag{2.20}$$

$$K = \sum_{i=n}^{n+N}\left(|y_{2i}|^2 + |y_{2i+1}|^2 + |\alpha_1|^2 + |\alpha_2|^2\right). \tag{2.21}$$

Then we have

$$\|\boldsymbol{y}_n - \boldsymbol{X}_n\boldsymbol{\alpha}\|^2 = K - 2|\eta_1|r_1\cos(A_1+\theta_1) - 2|\eta_2|r_2\cos(A_2-\theta_2), \tag{2.22}$$

where $\theta_i = \angle\alpha_i$, $r_i = |\alpha_i|$ and $A_i = \angle\eta_i$, $i = 1, 2$. Taking the Rayleigh fading assumption, we have θ uniformly distributed from $-\pi$ to π, and $r_i = |\alpha_i|$ Rayleigh distributed from 0 to ∞. Therefore,

$$\begin{aligned}\mathrm{p}(\boldsymbol{y}_n|\boldsymbol{X}_n, r_1, r_2) &= \int_{-\pi}^{\pi}\int_{-\pi}^{\pi}\mathrm{p}(\boldsymbol{y}_n|\boldsymbol{X}_n,\boldsymbol{\alpha})\mathrm{p}(\theta_1)\mathrm{p}(\theta_2)d\theta_1 d\theta_2,\\ &= \frac{1}{(\pi\sigma^2)^{2N}}\quad\exp\left(\frac{-K}{\sigma^2}\right)\\ &\quad \times I_0\left(\frac{2r_1|\eta_1|}{\sigma^2}\right)\times I_0\left(\frac{2r_2|\eta_2|}{\sigma^2}\right),\end{aligned} \tag{2.23}$$

where $I_0(.)$ is the zeroth order modified Bessel function of the first kind given by

$$I_0(x) = \sum_{k=0}^{\infty} \frac{1}{(k!)^2} x^{2k}, \quad i = 1, 2. \tag{2.24}$$

Yielding,

$$\mathrm{p}(\boldsymbol{y}_n|\boldsymbol{X}_n) = \int_0^{\infty}\int_0^{\infty} \mathrm{p}(\boldsymbol{y}_n|\boldsymbol{X}_n, r_1, r_2)\mathrm{p}(r_1)\mathrm{p}(r_2)dr_1dr_2, \tag{2.25}$$

where

$$\mathrm{p}(r) = \frac{\pi r}{2}\exp\left(\frac{-\pi r^2}{4}\right). \tag{2.26}$$

Substituting (2.23),(2.24) and (2.26) into (2.25), we obtain a sum of Gaussian integrals, which can be written as

$$\begin{aligned}
\mathrm{p}(\boldsymbol{y}_n|\boldsymbol{X}_n) &= \frac{1}{(\pi\sigma^2)^{2N}} \exp\left(\frac{-\sum_{i=n}^{n+N}\{|y_{2i}|^2 + |y_{2i+1}|^2\}}{\sigma^2}\right) \\
&\quad \times \frac{\pi}{4c}\exp\left(\frac{4|\eta_1|^2}{\sigma^4 c}\right) \times \frac{\pi}{4c}\exp\left(\frac{4|\eta_2|^2}{\sigma^4 c}\right) \\
&= \frac{1}{(\pi\sigma^2)^{2N}} \exp\left(\frac{-\sum_{i=n}^{n+N}\{|y_{2i}|^2 + |y_{2i+1}|^2\}}{\sigma^2}\right) \\
&\quad \times \left(\frac{\pi}{4}\right)^2 \exp\left(\frac{4(|\eta_1|^2 + |\eta_2|^2)}{\sigma^4 c}\right),
\end{aligned} \tag{2.27}$$

where $c = (\frac{N+1}{\sigma^2} + \frac{\pi}{4})$.

The ML receiver therefore is of the form

$$\begin{aligned}
\hat{\boldsymbol{X}}_n &= \arg\max_{\boldsymbol{X}} \left(|\eta_1|^2 + |\eta_2|^2\right). \\
&= \arg\max_{\boldsymbol{X}} \left\| \sum_{i=n}^{n+N} \underline{y}_i^H \underline{X}_i \right\|^2
\end{aligned} \tag{2.28}$$

where $\|.\|^2$ is the Frobenius norm and $\underline{y}_i$ is as defined in equation (2.15). Let,

$$\begin{aligned} \eta &= \left\| \sum_{i=n}^{n+N} \underline{y}_i^H \underline{X}_i \right\|^2 \\ &= \left\| \sum_{i=n}^{n+N} \underline{y}_i^H \boldsymbol{G}_i \underline{X}_n \right\|^2 \\ &= \left\| \sum_{i=n}^{n+N} \underline{y}_i^H \boldsymbol{G}_i \right\|^2 . \end{aligned} \tag{2.29}$$

where $\boldsymbol{G}_i = \prod_{j=n}^{i} \underline{G}_j$, and $\boldsymbol{G}_n = \boldsymbol{I}_2$. We choose $\boldsymbol{G}_{n+1}, \boldsymbol{G}_{n+2}, \cdots, \boldsymbol{G}_{n+N}$ as the ML estimates if they maximize η. Note that $\boldsymbol{G}_i \in \mathcal{G}$ defined in equation (2.5) and there are exactly $2M$ possible values that each $\boldsymbol{G}_i$ can take. M is defined in (2.1) and N is the window length. Hence the complexity of the solution to equation (2.28) based on an exhaustive search is $\mathcal{O}\left((2M)^N\right)$, which is prohibitive in practical applications for large values of N.

C. Fast STDC Decoding Algorithm

We propose a *"3 stage" fast algorithm* for finding the optimum solution to the above problem. Before going into the details of each stage, a brief overview of the functionalities will be helpful.

1: Find a good suboptimal initial estimate of $[\boldsymbol{G}_n \boldsymbol{G}_{n+1} \ldots \boldsymbol{G}_{n+N}]$.

2: Reduce the domain for each $\boldsymbol{G}_i$ from a maximum of $2M$ values to a lesser value.

3: Exact search algorithm based on a "*combine and bound*" method.

1. Stage 1

This stage finds a suboptimal estimate which will act as a lower bound for further stages, i.e., our search for an ML estimate will be reduced to only those sets $[\boldsymbol{G}_n \boldsymbol{G}_{n+1} \dots \boldsymbol{G}_{n+N}] \in \mathcal{G}^N$ which are better than this suboptimal estimate in terms of the magnitude of η.

Theorem 1 *Let* $\begin{bmatrix} \boldsymbol{G}_{0,n} & \boldsymbol{G}_{0,n+1} & \dots & \boldsymbol{G}_{0,n+N} \end{bmatrix}$ *maximize* η *over* $\mathcal{G}^N$. *Let* $\boldsymbol{Z}_i = \sum_{k \neq i} \underline{y}_k^H \boldsymbol{G}_k$ *for all* $n \leq i \leq n+N$. *Then*

$$\boldsymbol{G}_{0,i} = \arg \max_{\boldsymbol{G}_i \in \mathcal{G}} \left\| \underline{y}_i^H \boldsymbol{G}_i + \boldsymbol{Z}_i \right\|^2. \tag{2.30}$$

Proof: We prove this theorem by contradiction. Suppose there exists an $\boldsymbol{G}_{l,i} \in \mathcal{G}$ *other than* $\boldsymbol{G}_{0,i}$, *such that*

$$\boldsymbol{G}_{l,i} = \arg \max_{\boldsymbol{G}_i \in \mathcal{G}} \left\| \underline{y}_i^H \boldsymbol{G}_i + \boldsymbol{Z}_i \right\|^2, \tag{2.31}$$

then, $\left\| \underline{y}_i^H \boldsymbol{G}_{l,i} + \boldsymbol{Z}_i \right\|^2 > \left\| \underline{y}_i^H \boldsymbol{G}_{0,i} + \boldsymbol{Z}_i \right\|^2$.

This contradicts our assumption that $[\boldsymbol{G}_n \boldsymbol{G}_{n+1} \dots \boldsymbol{G}_{n+N}]$ *maximizes* η. *Hence Proved.*

Based on this theorem, we will iteratively compute a suboptimal initial estimate as given below.

Algorithm 2 (Fast MS-STDC Decoding Algorithm - Stage 1) *We, start by picking the* $\boldsymbol{G}_i$*'s randomly from* $\mathcal{G}$ *for all* $n \leq i \leq n+N$.

1. *Set the loop test condition "flag = 0".*

2. *For all* $n \leq i \leq n+N$.

   - *Calculate* $\boldsymbol{Z}_i$ *and over all* $\boldsymbol{G}_i \in \mathcal{G}$, *find the one that maximizes* η.

   - *If the value of* η *is changed, set "flag=1".*

3. *If "flag" is set to 1, repeat steps 1 and 2. This loop iteratively arrives at an estimate* $[\boldsymbol{G}_{l,n}\boldsymbol{G}_{l,n+1}\ldots\boldsymbol{G}_{l,n+N}]$ *which satisfies equation (2.30).*

4. *Calculate* $\eta_l = \left\|\sum_{i=n}^{n+N} \underline{y}_i^H \boldsymbol{G}_i\right\|^2$.

The η_l thus arrived at will be used as a lower bound for the future calculations.

2. Stage 2

The domain $\mathcal{G}_i \in \mathcal{G}$ for each $\boldsymbol{G}_i$, $n \leq i \leq n+N$ has $2M$ elements. We wish to reduce this domain space to a smaller set to simplify further calculations. Before doing that, we propose a method to find a tight upper-bound for η

$$\begin{aligned}
\eta &= \left\|\sum_{i=n}^{n+N} \underline{y}_i^H \boldsymbol{G}_i\right\|^2, \\
&= \sum_{i=n}^{n+N} \left(|y_{2i}|^2 + |y_{2i+1}|^2\right) + 2\Re \sum_{i=n}^{n+N-1} \sum_{j=i+1}^{n+N} \underline{y}_i^H \boldsymbol{G}_i \boldsymbol{G}_j^H \underline{y}_j, \\
&= \sum_{i=n}^{n+N} \left(|y_{2i}|^2 + |y_{2i+1}|^2\right) + \sum_{i=n}^{n+N-1} \sum_{j=i+1}^{n+N} \eta_{ij}. \qquad (2.32)
\end{aligned}$$

where $\eta_{ij} = 2\Re(\underline{y}_i^H \boldsymbol{G}_i \boldsymbol{G}_j^H \underline{y}_j)$. To compute an upper bound η_u for η, we individually maximize each η_{ij} in (2.32), choosing $\boldsymbol{G}_i \in \mathcal{G}_i$ and $\boldsymbol{G}_j \in \mathcal{G}_j$.

$$\eta_u = \sum_{i=n}^{n+N} \left(|y_{2i}|^2 + |y_{2i+1}|^2\right) + \sum_{i=n}^{n+N-1} \sum_{j=i+1}^{n+N} \max_{\boldsymbol{G}_i \in \mathcal{G}_i, \boldsymbol{G}_j \in \mathcal{G}_j} (\eta_{ij}). \qquad (2.33)$$

It is seen that the calculation of η_u is much easier compared to calculating $\max \eta$.

A conditional upper bound is defined as an upper bound calculated when the domain $\mathcal{G}^N$ is reduced or bounded in some way, e.g, some of the $\boldsymbol{G}_i$ are already set to a certain value. We can now discuss the Algorithm for *iteratively* reducing the constellations $\mathcal{G}_i$.

Algorithm 3 (Fast MS-STDC Decoding Algorithm - Stage 2) *Set* $\mathcal{G}_n = \{\boldsymbol{I}_2\}$.

For $n \leq i \leq n+N$, *initialize* $\mathcal{G}_i = \mathcal{G}$. *Define* c_i *as the number of elements in* $\mathcal{G}_i$.

1. *Set the loop test condition "flag = 0".*
2. *For* $i = n+1, \ldots, n+N$.
   - *For* $k = 1, \ldots, c_i$.
     - *Fix* $\boldsymbol{G}_i = \boldsymbol{G}_{i,k}$, *where* $\boldsymbol{G}_{i,k}$ *is the* k^{th} *element in* $\mathcal{G}_i$.
     - *If the conditional upper bound* η_u *is less than* η_l,
       - *Remove* $\boldsymbol{G}_{i,k}$ *from* $\mathcal{G}_i$, *update* $c_i = c_i - 1$, *Set "flag=1".*
3. *If "flag=1", repeat 1 & 2. This loop will iteratively reduce all the constellations.*

3. Stage 3

The problem now reduces to finding an ML estimate, choosing $\boldsymbol{G}_i \in \mathcal{G}_i$ for all $n \leq i \leq n+N$. An exhaustive search will still have a large complexity proportional to $c_n c_{n+1} \ldots c_{n+N}$. We propose a "combine and bound" algorithm to search for a ML estimate with a reduced complexity.

Stage 2 ensures that choosing any $\boldsymbol{G}_i \in \mathcal{G}_i$ for any i results in a conditional upper bound $\eta_u \geq \eta_l$. What happens if we fix both $\boldsymbol{G}_n$ and $\boldsymbol{G}_{n+1}$ simultaneously choosing from $\mathcal{G}_n$ and $\mathcal{G}_{n+1}$ respectively? There can be a total possible of $c_n c_{n+1}$ combinations for choosing $[\boldsymbol{G}_n \;\; \boldsymbol{G}_{n+1}]$. Not all of these will lead to a conditional upper bound $\eta_u \geq \eta_l$. The irrelevant combinations therefore have to be removed.

This notion leads to the concept of a joint constellation $\mathcal{G}_{n,n+1}$ for $[\boldsymbol{G}_n \;\; \boldsymbol{G}_{n+1}]$, which can be formed by combining $\mathcal{G}_n$ and $\mathcal{G}_{n+1}$ as described below.

$$\begin{aligned} \mathcal{G}_{n,n+1} &= \mathcal{G}_n \times \mathcal{G}_{n+1} \\ &= \left\{ \begin{bmatrix} \boldsymbol{G}_{n,p} & \boldsymbol{G}_{n+1,q} \end{bmatrix}, 1 \leq p \leq c_n, 1 \leq q \leq c_{n+1} \right\} \end{aligned} \tag{2.34}$$

Note that $\mathcal{G}_{n,n+1}$ has exactly $c_n c_{n+1}$ elements. Let $\boldsymbol{D}^p_{n,n+1}$ be the p^{th} element of $\mathcal{G}_{n,n+1}$. Remove $\boldsymbol{D}^p_{n,n+1}$ from the set if upon fixing $[\boldsymbol{G}_n \;\; \boldsymbol{G}_{n+1}] = \boldsymbol{D}^p_{n,n+1}$, the upper bound $\eta_u < \eta_l$. Let $c_{n,n+1}$ be the number of elements remaining in $\mathcal{G}_{n,n+1}$. Similarly, a joint constellation set $\mathcal{G}_{n+2,n+3}$ for $[\boldsymbol{G}_{n+2} \;\; \boldsymbol{G}_{n+3}]$ can be formed.

What happens if we fix $[\boldsymbol{G}_n \;\; \boldsymbol{G}_{n+1} \;\; \boldsymbol{G}_{n+2} \;\; \boldsymbol{G}_{n+3}]$ simultaneously? We need to find a joint constellation $\mathcal{G}_{n,n+1,n+2,n+3}$. For simplicity of notation we can write it as $\mathcal{G}_{n,n+3}$ noting only the starting variable and the ending variable index.

$$\begin{aligned} \mathcal{G}_{n,n+3} &= \mathcal{G}_{n,n+1} \times \mathcal{G}_{n+2,n+3} \\ &= \left\{ \begin{bmatrix} \boldsymbol{D}^p_{n,n+1} & \boldsymbol{D}^q_{n+2,n+3} \end{bmatrix}, \; 1 \leq p \leq c_{n,n+1}, \; 1 \leq q \leq c_{n+2,n+3} \right\} \end{aligned} \tag{2.35}$$

Let $\boldsymbol{D}^p_{n,n+3}$ be the p^{th} element in $\mathcal{G}_{n,n+3}$. Remove $\boldsymbol{D}^p_{n,n+3}$ from the set if upon fixing $[\boldsymbol{G}_n \;\; \boldsymbol{G}_{n+1} \;\; \boldsymbol{G}_{n+2} \;\; \boldsymbol{G}_{n+3}] = \boldsymbol{D}^p_{n,n+3}$, the upper bound $\eta_u < \eta_l$.

We wish to finally form a joint constellation $\mathcal{G}_{n,n+N}$. The elements $\boldsymbol{D}_{n,n+N} \in \mathcal{G}_{n,n+N}$ are realizations for $[\boldsymbol{G}_n \;\; \boldsymbol{G}_{n+1} \;\; \ldots \;\; \boldsymbol{G}_{n+N}]$. An efficient algorithm for finding $\mathcal{G}_{n,n+N}$ is recursive and can be best understood using the following "pseudo" code.

```
main()
{
    ⋮
    G=makeG(n,n+N);                    // G is the joint constellation G_{n,n+N}.
    ⋮
}
makeG(i,j)
{
    if (j>i)
    {
        k=midpoint(i,j);
        G1=makeG(i,k);                 // G1 is the joint constellation G_{i,k}
        G2=makeG(k+1,j);               // G2 is the joint constellation G_{k+1,j}
        G=combine(G1,G2);              // G is the joint constellation G_{i,j}
    }
    else if (i==j)
        G=Const[i];                    // G is the constellation G_i
    return G;
}
```

The function combine() is as described in the above paragraphs. The joint constellation $\mathcal{G}_{n,n+N}$ is formed in the function main().

We now have the following algorithm for computing the ML estimate.

Algorithm 4 (Fast Multiple-Symbol STDC decoding Algorithm - Stage 3)

From stage 2 we have $\mathcal{G}_i$'s for $n \leq i \leq n+N$.

- *Combine them to form* $\mathcal{G}_{n,n+N}$ *using the pseudo code given above.*

- *Find a* $\left[\hat{\boldsymbol{G}}_n \;\; \hat{\boldsymbol{G}}_{n+1} \ldots \hat{\boldsymbol{G}}_{n+N}\right] \in \mathcal{G}_{n,n+N}$*, which maximizes the* η*.*

- *Form* $\underline{\hat{A}}_i = \boldsymbol{G}_i \boldsymbol{G}_{i-1}^H \underline{A}_0$*, where* $\underline{A}_0$ *is the pilot symbol sent at the beginning.*

CHAPTER III

ITERATIVE DECODING OF DIFFERENTIALLY SPACE-TIME CODED MULTIPLE DESCRIPTIONS OF IMAGES

As described in chapter I, we propose a serial concatenation of a JSCC and a STDC code (section A). Sections B and C describe the maximum *a posteriori* probability (MAP) STDC decoder and the SPIHT + RCPC/CRC decoder respectively.

A. Iterative Decoding

We consider an MD source code using SPIHT + RCPC/CRC and a STDC with two transmit antennas and one receive antenna. The former can be viewed as an effective source code (with robustness to channel errors), while the latter an effective channel code. We thus propose a serial concatenation of these two (see Fig. 2) and employ an iterative decoding technique for differential space-time coded multiple descriptions (STDC-MD).

Our proposed receiver consists of a MAP STDC decoder [8], an MD source decoder, an interleaver and a de-interleaver. The two decoders exchange the *a priori* probabilities of transmitted bits between themselves in successive iterations. These *a priori* probabilities are also known as the extrinsic values. The inputs to the STDC decoder are the channel values and the *a priori* probabilities. This MAP decoder calculates the log likelihood ratio [1] (LLR) for each information bit and passes it on as the output. These values are then de-interleaved to bring them in the right order for the MD source decoder. The interleaving is done at the transmitter to counter the effect of burst errors which are common in fading channels. Using these inputs, the

[1] defined in section B

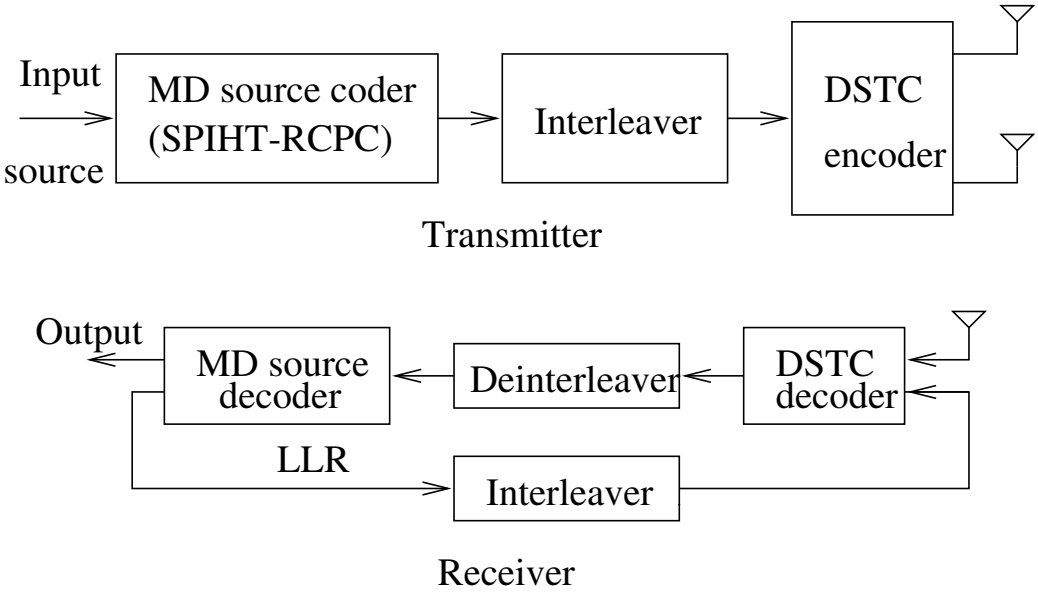

Fig. 2. The proposed serial concatenation of MD coding and differential STC.

MD source decoder calculates the extrinsic values, which are interleaved and passed to the MAP STDC decoder. The MD source decoder employs a log-MAP algorithm to calculate the extrinsic values to be passed on to the next stage. At the last iteration, however, the MD source decoder employs a list decoding technique. The best estimate in the "list" which satisfies the CRC check is chosen.

B. MAP STDC Decoding in Fading Channel

We consider a flat-fading channel, where the fading processes associated between a transmit and a receive antenna can be denoted by α_t as a function of time t. These processes are modelled as mutually independent complex Gaussian variables with Jakes' correlation structure [24]. Each of them has normalized autocorrelation

function

$$R(n) = E\{\alpha_{t+n}\alpha_t\} = E_s J_0(2\pi B_d n T). \tag{3.1}$$

where, E_s is the average energy, $J_0(.)$ is the zeroth order Bessel function of the first kind, T is the symbol interval, and B_d is the maximum Doppler shift. We assume that the channel remains constant over a block of two consecutive symbols. Consider the system described in chapter II, section A. Let α_{1i} and α_{2i} be the complex fading gains between the two transmit antennas and the receive antenna, respectively. The received signals are then given respectively by

$$\underbrace{\begin{bmatrix} y_{2i} \\ y_{2i+1} \end{bmatrix}}_{\underline{y}_i} = \underbrace{\begin{bmatrix} x_{2i} & x_{2i+1} \\ -x_{2i+1}^* & x_{2i}^* \end{bmatrix}}_{\underline{X}_i} \underbrace{\begin{bmatrix} \alpha_{1i} \\ \alpha_{2i} \end{bmatrix}}_{\boldsymbol{\alpha}_i} + \underbrace{\begin{bmatrix} v_{2i} \\ v_{2i+1} \end{bmatrix}}_{\boldsymbol{v}_i}. \tag{3.2}$$

where v_{2i} and v_{2i+1} are independent zero-mean symmetric complex Gaussian noise samples with variance σ^2.

A MAP decoding algorithm was developed in [8] using the trellis representation. The trellis has $2M$ states corresponding to the values that $\underline{X}_i$ can take. There are $2M$ branches going out of and coming into each state corresponding to the values of $\underline{A}_i$. Further, each branch is a vector consisting of exactly $\log_2 M + 1$ bits.

The inputs to the decoder are the channel output vector $\boldsymbol{y}_n$ and the *a priori* probabilities or the extrinsic values $L(d_i(k))$ of the bits. The decoder calculates the *a posteriori* probability (APP) or the log likelihood ratio (LLR) of each bit as

$$\Lambda(d_i(k)) = \log\left(\frac{\mathrm{p}\ (d_i(k) = 1|\boldsymbol{y}_n)}{\mathrm{p}\ (d_i(k) = 0|\boldsymbol{y}_n)}\right), \tag{3.3}$$

where $d_i(k)$ is the k-th of the $\log_2 M + 1$ bits of the i-th input vector. The APP can be written in terms of the transition probabilities of the trellis. Following [8], we define a set of all state transitions corresponding to the input bit $d_i(k) = q$ as

$$B_{d_i(k)=q} = \{(m', m) : d_i(k) = q, S_{i-1} = m', S_i = m\}, \tag{3.4}$$

where S_i denotes the state on the trellis at time i and m is the value that S_i takes. The LLR is defined as

$$\Lambda(d_i(k)) = \log \frac{\sum_{(m',m)\in B_{d_i(k)=1}} \sigma_i(\boldsymbol{y}_n, m', m)}{\sum_{(m',m)\in B_{d_i(k)=0}} \sigma_i(\boldsymbol{y}_n, m', m)}\ , \tag{3.5}$$

where $\sigma_i(\boldsymbol{y}_n, m', m)$ is the probability that a transition from state m' to m occurs at i and can be written as

$$\sigma_i(\boldsymbol{y}_n, m', m) = \alpha_{i-1}(m')\gamma_i(m', m)\beta_i(m), \tag{3.6}$$

with $\alpha_i(m)$ and $\beta_i(m)$ being the probabilities that S_i is m. They can be calculated recursively as

$$\alpha_i(m) \;=\; \sum_{m'} \alpha_{i-1}(m')\gamma_i(m', m), \tag{3.7}$$

$$\beta_i(m) \;=\; \sum_{m'} \beta_{i+1}(m')\gamma_{i+1}(m, m'). \tag{3.8}$$

The inner decoder transition metric between m' and m is given by

$$\begin{aligned} \gamma_i(m', m) &= \mathrm{p}(\underline{A}_i)\mathrm{p}(\underline{y}_i|\underline{X}_i) \\ &= \left(\prod_{k=1}^{\log_2 M+1} \mathrm{p}\ (d_i(k) = q)\right) \mathrm{p}\left(\underline{y}_i|\underline{X}_i\right). \end{aligned} \tag{3.9}$$

where p $(d_i(k))$ are the *a-priori* probabilities. These probabilities are calculated from the extrinsic information of the outer decoder denoted as $L(d_i(k))$.

For estimating $\mathrm{p}(\underline{y}_i|\underline{X}_i)$, we first estimate $\boldsymbol{\alpha}_i$ using the per-survivor processing [25] and the linear prediction. We can write

$$\mathrm{p}(\underline{y}_i|\underline{X}_i\underline{\alpha}_i) \propto \exp\left(-\frac{\| \underline{y}_i - \underline{X}_i\underline{\alpha}_i \|^2}{\sigma^2}\right). \tag{3.10}$$

The perfect $\underline{\alpha}_i$ is not known, so it is replaced by an estimate $\hat{\underline{\alpha}}_i$, which is obtained by linear prediction as

$$\hat{\underline{\alpha}}_i = \sum_{l=1}^{P} \omega_l \widetilde{\underline{\alpha}}_{i-l}, \tag{3.11}$$

where P is the predictor length and ω_l are its coefficients. $\widetilde{\underline{\alpha}}_{i-l}$ are the previous channel estimates obtained using the per survivor principle $\widetilde{\underline{\alpha}}_{i-l} = \underline{X}_{i-l}^H \underline{y}_{i-l}$. Therefore , the metric of the received signal is

$$\mathrm{p}(\underline{y}_i|\underline{X}_i) \propto \exp\left(\frac{-1}{\sigma^2}\left\|\underline{y}_i - \underline{X}_i \sum_{l=1}^{P} \omega_l \underline{X}_{i-l}^H \underline{y}_{i-l}\right\|^2\right). \tag{3.12}$$

We choose $P = 1$ and $\omega_1 = 1$ for our simulations. The metric becomes,

$$\mathrm{p}(\underline{y}_i|\underline{X}_i) \propto \exp\left(\frac{-1}{\sigma^2}\left\|\underline{y}_i - \underline{X}_i\underline{X}_{i-1}^H\underline{y}_{i-1}\right\|^2\right). \tag{3.13}$$

The extrinsic values that are passed onto the next stage are calculated as

$$L_e(d_i(k)) = \Lambda(d_i(k)) - L(d_i(k)). \tag{3.14}$$

Algorithm 5 (MAP Decoding Algorithm for Multiple-Symbol STDC) *The following is a MAP decoding algorithm for STDC without requiring the CSI.*

- *Calculate the $\alpha_i(m), \beta_i(m)$ and $\gamma_i(m', m)$ for each state and time using the Equations (3.7),(3.8) and (3.9).*

- *Calculate the path transition probabilities for each path using the relation*

$$\sigma_i(m', m) = \alpha_{i-1}(m')\gamma_i(m', m)\beta_i(m). \tag{3.15}$$

- *Calculate the LLR for each bit using (3.5).*

- *Calculate the extrinsic values using (3.14) from these LLR values.*

Fig. 3 shows the BER performance of MAP differential space-time decoding with a normalized Doppler f_aT=0.01. The decoding window length is 216 and the 8-PSK constellation is used for transmitting symbols. Fig. 4 shows the performance of a serially concatenated system of a MAP STDC decoder and a simple rate 1/2 convolution code.

C. MD Source Coding with List Viterbi Decoding

1. SPIHT

SPIHT is a powerful wavelet-based image compression method optimized for progressive image transmissions (like WWW browsers). SPIHT coding converts an image file into a stream of bits in such a fashion that if there are two encoded files of sizes M and N bits respectively and if $N > M$, then the first M bits of both the files are identical. The SPIHT achieves superior results than most schemes by using a simpler method of uniform scalar quantization. Also, the compression simplicity directly implies faster coding and decoding.

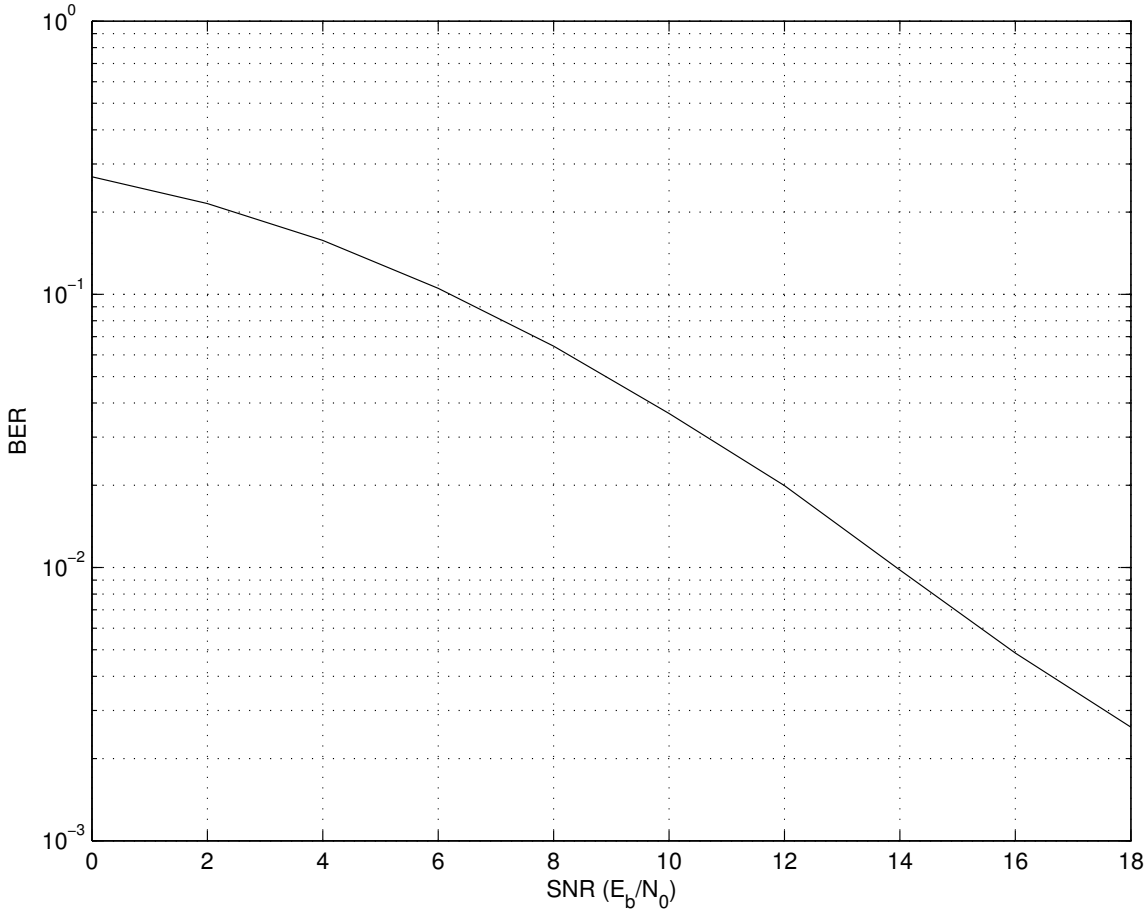

Fig. 3. Performance of MAP differential space-time decoding in a fading channel with a normalized Doppler f_aT=0.01.

2. List decoding of RCPC/CRC

The CRC is used to protect blocks of data (Frames). The transmitter adds an extra n parity bit sequence to every frame based on a generator polynomial. These extra bits hold redundant information about the frame and help detect errors at the receiver.

RCPC codes are generated by puncturing a rate $\frac{1}{R}$ convolutional code periodically with a period P to obtain a family of codes with rate $\frac{P}{P+l}$ where l can be varied between 1 and $(N-1)P$. For our simulations, we used a rate $\frac{1}{6}$ convolution code

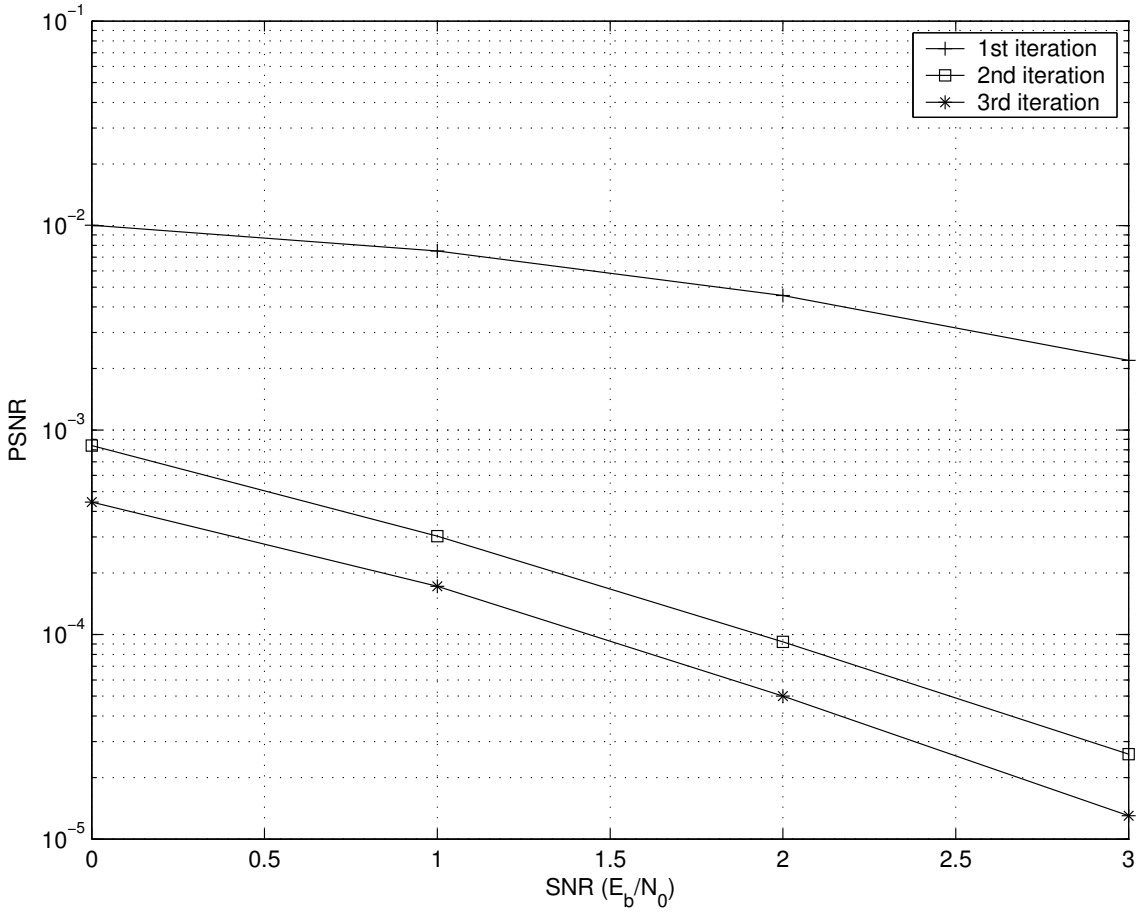

Fig. 4. Performance of MAP differential space-time decoding concatenated with a rate 1/2 convolution code in a fading channel with a normalized Doppler f_aT=0.01.

with 6 memory elements and deleted the output bits periodically to set the rate to the required value. More details about these codes can be found in [20].

For the decoding of the RCPC codes we use a log-MAP decoding algorithm similar to the one developed in [9] using the trellis representation. The trellis has 2^k states corresponding to each of the states of the $k-1$ memory elements. Each state has 2 branches going out of and coming into it. These branches correspond to the binary values that the input information bit can take. Further, each branch between

two nodes consists of exactly R bits, in other words it has information about exactly 1 *input* bit.

The inputs to the decoder are the *a priori* probabilities or the extrinsic values $L(d_k(i))$ of the bits, where $d_k(i)$ is the i-th of the R output bits corresponding to the k-th input information bit. The decoder has two kinds of outputs

- In the last iteration, the decoder gives the estimates for the information bits.
- In all other iterations, the decoder produces the log likelihood ratios (LLR) of each of the constituent R bits.

Lets first discuss the latter, the LLR or the *a posteriori* probabilities are best described according to the following equation.

$$\Lambda(d_k(i)) = \log\left(\frac{\mathrm{p}(d_k(i)=1)}{\mathrm{p}(d_k(i)=0)}\right) \tag{3.16}$$

The APP can be written in terms of the transition probabilities of the trellis. We define a set of all state transitions corresponding to the bit $d_k(i) = q$ as

$$B_{d_k(i)=q} = \{(m', m) : d_k(i) = q, S_{k-1} = m', S_k = m\} \tag{3.17}$$

where S_k denotes the state on the trellis at time k and m, and m' are the values that S_k takes. We now define the LLR as

$$\Lambda(d_k(i)) = \log\frac{\sum_{(m',m)\in B_{d_k(i)=1}} \sigma_k(m', m)}{\sum_{(m',m)\in B_{d_k(i)=0}} \sigma_k(m', m)} \tag{3.18}$$

where $\sigma_k(m', m)$ is the probability that a transition from state m' to m occurs at k and can be written as

$$\sigma_k(m', m) = \alpha_{k-1}(m')\gamma_k(m', m)\beta_k(m) \tag{3.19}$$

with $\alpha_k(m)$ and $\beta_k(m)$ being the probabilities that the state at time k is m. They can be calculated recursively as

$$\alpha_k(m) = \sum_{m'} \alpha_{k-1}(m')\gamma_k(m', m), \tag{3.20}$$

$$\beta_k(m) = \sum_{m'} \beta_{k+1}(m')\gamma_{k+1}(m, m') \tag{3.21}$$

The transition metric between m' and m is given by

$$\gamma_k(m', m) = \prod_{i=1}^{N} \mathrm{p}(d_k(i) = q). \tag{3.22}$$

where $\mathrm{p}(d_k(i))$ are the *a-priori* probabilities input to the decoder. These probabilities are calculated in the inner decoder as $L(d_k(i))$, and are passed onto the outer decoder through a deinterleaver.

The extrinsic values that are passed as outputs are simply calculated as

$$L_c(d_k(i)) = \Lambda(d_k(i)) - L(d_k(i)) \tag{3.23}$$

Algorithm 6 (log-MAP Decoding Algorithm for RCPC) *We can summarize the above discussion in terms of an algorithm as follows.*

- *For each state and time, compute* $\alpha_k(m)$, $\beta_k(m)$, $\gamma_k(m', m)$ *using (3.20,3.21,3.22).*
- *Calculate the transition probabilities* $\sigma_k(m', m) = \alpha_{k-1}(m')\gamma_k(m', m)\beta_k(m)$.
- *Calculate the LLR for each bit using (3.18).*
- *Calculate the extrinsic values using Equation (3.23) from these LLR values.*

A combination of RCPC + CRC is a very powerful technique to detect and

correct errors. In the last iteration, the parity bits from the CRC come into play. A *list-decoding* procedure is employed. The Viterbi algorithm is employed on the trellis structure already designed to provide a list of hard estimates for the sequence of input bits. The best path from the Viterbi occurs at the top of the list, while going down the list worsens the euclidean distance of the channel values from the estimate. From the list, the best estimate which satisfies the CRC check is picked as the final estimate. These estimates from all the frames are combined to form a bit stream which can be SPIHT decoded to form an image.

3. SPIHT + RCPC/CRC

The MD source coder can be simply based on MD correlating image transforms [12] or embedded coding (e.g., SPIHT) and UEP [14, 15]. An example of the latter case is given in Fig. 5 [10], where the embedded source coder (e.g., SPIHT) is employed to produce a rate $(2-\rho)R$ bitstream with $0 \leq \rho \leq 1$. The first ρR portion of the embedded bitstream is repeated in both descriptions, as indicated by the box, while the remaining $2(1-\rho)R$ portion are split between the two descriptions.

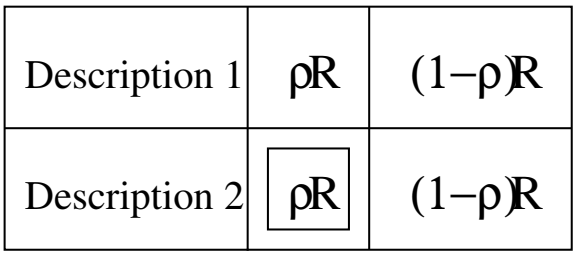

Fig. 5. Two descriptions generated with embedded coding and UEP.

In our work, because we are dealing with fading channels, we view both MD coding and JSCC as means of introducing redundancy into our communication system for

error robustness. Thus, conceptually any practical JSCC scheme with soft-threshold channel coding can be employed as the MD coder in our system. Since Sherwood and Zeger showed the effectiveness of their simple SPIHT+RCPC/CRC scheme in [19], many works have been done on JSCC for scalable multimedia transmission over both binary symmetric channels (BSC) and packet erasure channels. In this work, we choose the SPIHT+RCPC/CRC scheme for MD coding (or JSCC) due to its good performance even though it is based on equal error protection. Other UEP-based practical JSCC schemes (e.g., [26]) may also be used in our system.

The performance of the MD source decoder obviously depends on the amount of redundancy introduced in the RCPC code. For a given channel condition (e.g., SNR) and transmission rate, we choose the RCPC code rate to maximize the system performance with a fixed number of iterations.

CHAPTER IV

ITERATIVE DECODING OF SPACE-TIME CODED MULTIPLE DESCRIPTIONS OF IMAGES

The performance of the system developed in the chapter III is compared against a serial concatenation of a SPIHT + RCPC/CRC with an STC as opposed to an STDC. At the receiver, two schemes are considered, one in which the receiver has perfect CSI and the other in which pilot symbols are used to estimate the CSI. A MAP decoding algorithm based on the Expectation-Maximization (EM) principle has been developed in [22] for OFDM systems. It is modified for flat fading channels. Section A describes the MAP decoder for the STC.

A. MAP Space-Time Decoding in Fading Channel

Consider a communication system with two transmit antennas and one receive antenna. Let the M-ary PSK (M-PSK) symbols at time $2i$ and $2i+1$ be

$$a_{2i}, a_{2i+1} \in \mathcal{A} \triangleq \left\{ \frac{1}{\sqrt{2}} e^{j\frac{2\pi k}{M}},\ k = 0, 1, \cdots, M-1 \right\}. \tag{4.1}$$

Define the matrix:

$$\underline{A}_i \triangleq \begin{bmatrix} a_{2i} & a_{2i+1} \\ -a_{2i+1}^* & a_{2i}^* \end{bmatrix},\ \text{for } i \geq 0, \tag{4.2}$$

It is easy to see that $\underline{A}_i$ is an orthogonal matrices, i.e., $\underline{A}_i \underline{A}_i^H = \underline{A}_i^H \underline{A}_i = \boldsymbol{I}_2$.

At time slot $2i$, the symbols on the first row of $\underline{A}_i$ in (4.2), a_{2i} and a_{2i+1} are transmitted simultaneously from antenna 1 and antenna 2, respectively. At time slot $2i+1$, the symbols on the second row of $\underline{A}_i$, $-a_{2i+1}^*$ and a_{2i}^* are transmitted

simultaneously from the two antennas. We consider a fast fading channel which remains constant for the transmission of a single space-time matrix. Let α_{1i} and α_{2i} be the complex fading gains at the transmission of the i^{th} matrix between the two transmit antennas and the receive antenna, respectively. The received signals are,

$$\underbrace{\begin{bmatrix} y_{2i} \\ y_{2i+1} \end{bmatrix}}_{\underline{y}_i} = \underbrace{\begin{bmatrix} a_{2i} & a_{2i+1} \\ -a^*_{2i+1} & a^*_{2i} \end{bmatrix}}_{\underline{A}_i} \underbrace{\begin{bmatrix} \alpha_{1i} \\ \alpha_{2i} \end{bmatrix}}_{\underline{\alpha}_i} + \underbrace{\begin{bmatrix} v_{2i} \\ v_{2i+1} \end{bmatrix}}_{\underline{v}_i}. \tag{4.3}$$

where v_{2i} and v_{2i+1} are independent zero-mean symmetric complex Gaussian noise samples with variance σ^2

We modify the trellis based MAP decoding algorithm for STDC to suite the STC. The inputs to the decoder are the channel output vector $\underline{y}_i$ and the *a priori* probabilities or the extrinsic values $L(d_i(k))$ of the bits. The decoder calculates the *a posteriori* probability (APP) or the log likelihood ratio (LLR) of each bit as

$$\Lambda(d_i(k)) = \log\left(\frac{\mathrm{p}(d_i(k)=1|\underline{y}_i)}{\mathrm{p}(d_i(k)=0|\underline{y}_i)}\right) \tag{4.4}$$

where $d_i(k)$ is the k-th of the $2\log_2 M$ information bits of the i-th input vector. The APP can be written in terms of the transition probabilities of the trellis. Following [8], we define a set of all state transitions corresponding to the input bit $d_i(k) = q$ as

$$B_{d_i(k)=q} = \{m : d_i(k) = q, \underline{A}_i = m\} \tag{4.5}$$

where m is a value that $\underline{A}_i$ takes out of the M^2 values in the constellation. The LLR

is defined as

$$\Lambda(d_i(k)) = \log \frac{\sum_{m \in B_{d_i(k)=1}} \gamma_i(m)}{\sum_{m \in B_{d_i(k)=0}} \gamma_i(m)} \tag{4.6}$$

where $\gamma_n(m)$ is the probability that $\underline{A}_i = m$. The inner decoder transition metric is given by

$$\begin{aligned} \gamma_i(m) &= \mathrm{p}(\underline{A}_i)\mathrm{p}(\underline{y}_i|\underline{A}_i) \\ &= \left(\prod_{k=1}^{2\log_2 M} \mathrm{p}(d_i(k) = q) \right) \mathrm{p}\left(\underline{y}_i|\underline{A}_i\right). \end{aligned} \tag{4.7}$$

where $\mathrm{p}(d_i(k))$ are the *a-priori* probabilities. These probabilities are calculated from the extrinsic information of the outer decoder denoted as $L(d_i(k))$.

For estimating $\mathrm{p}(\underline{y}_i|\underline{A}_i)$, we first estimate $\underline{\alpha}_i$. We consider two approaches,

- Perfect Channel State Information (CSI) at the Receiver.
- Estimate using a pilot symbol coupled with a per survivor prediction approach.

We can write

$$\mathrm{p}(\underline{y}_i|\underline{A}_i\underline{\alpha}_i) \propto \exp\left(-\frac{\| \underline{y}_i - \underline{A}_i\underline{\alpha}_i \|^2}{\sigma^2} \right) \tag{4.8}$$

When perfect CSI is available, i.e., $\underline{\alpha}_i$ is known at the receiver, the computation of $\mathrm{p}(\underline{y}_i|\underline{A}_i)$ becomes straightforward.

When the perfect $\underline{\alpha}_i$ is not known, we can replace it by an estimate of it.

$$\hat{\underline{\alpha}}_i = \underline{A}_{i-1}^H \underline{y}_{i-1} \tag{4.9}$$

where, $\underline{A}_{i-1}$ which has the maximum $\mathrm{p}(\underline{y}_{i-1}|\underline{A}_{i-1})$ is chosen among the possible M^2

values. We can therefore write

$$\mathrm{p}(\underline{y}_i|\underline{A}_i) = \exp\left(\frac{-1}{\sigma^2}\left\|\underline{y}_i - \underline{A}_i\underline{A}_{i-1}^H\underline{y}_{i-1}\right\|^2\right) \tag{4.10}$$

Once this has been done, the extrinsic values that are passed onto the next stage can be simply calculated as

$$L_e(d_i(k)) = \Lambda(d_i(k)) - L(d_i(k)) \tag{4.11}$$

We therefore arrive at the following MAP algorithm.

Algorithm 7 (MAP Decoding Algorithm for STC) *The following is a MAP decoding algorithm for space-time codes.*

- *Calculate the $\gamma_i(m)$ for each time and path using the equation (4.7).*
- *Calculate the LLR for each bit using (4.6).*
- *Calculate the extrinsic values using (4.11) from these LLR values.*

Fig. 6 shows the BER performance of MAP STC decoder in a fading channel w¡ith a normalized Doppler f_aT=0.01. The window length is 216. Both the cases of perfect CSI at the receiver and linear prediction are shown.

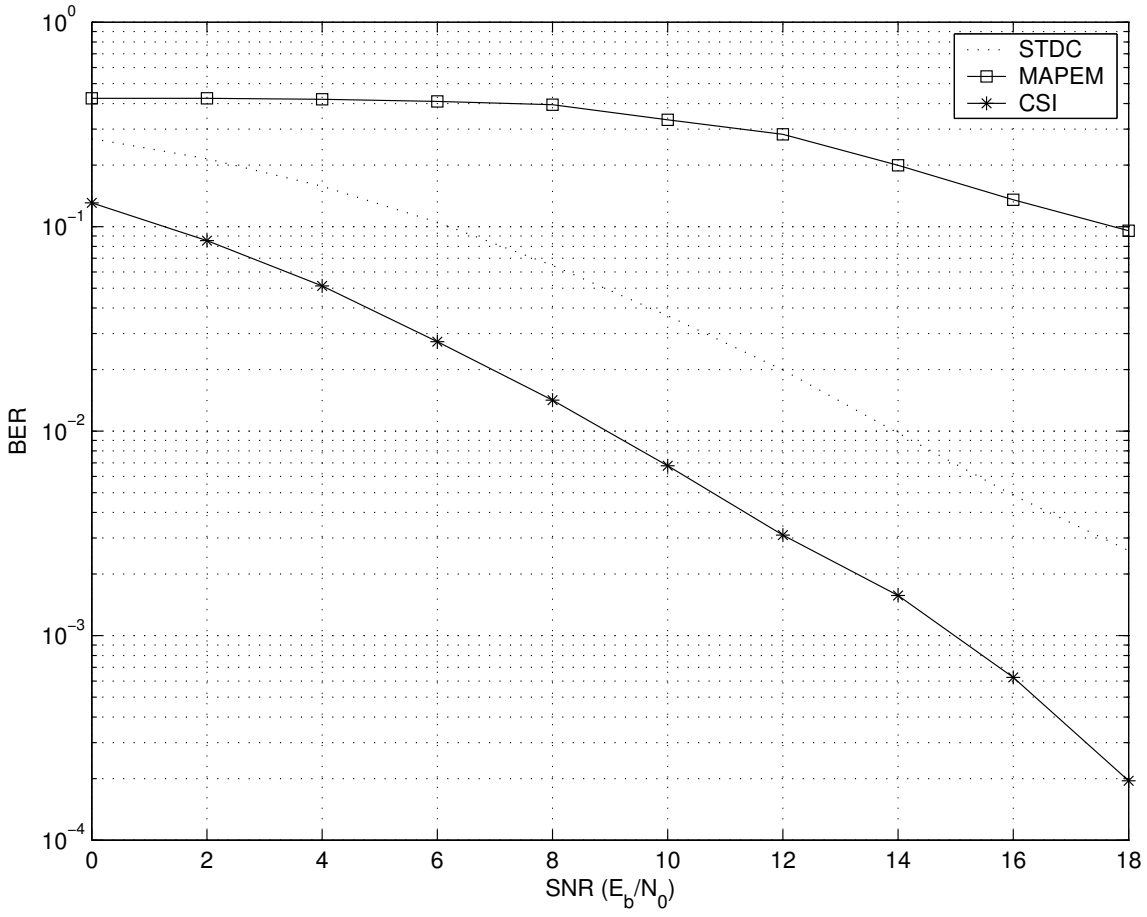

Fig. 6. Performance of MAP STC decoding with a normalized Doppler f_aT=0.01.

CHAPTER V

RESULTS AND CONCLUSION

This chapter presents the results and conclusions for the systems and algorithms designed in the preceding chapters. Section A discusses the performance results of the fast algorithm. The simulation results for the proposed concatenation of STDC with SPIHT + RCPC/CRC system are given in section B. Finally, section C has the simulation results for the serial concatenation of STC with SPIHT + RCPC/CRC.

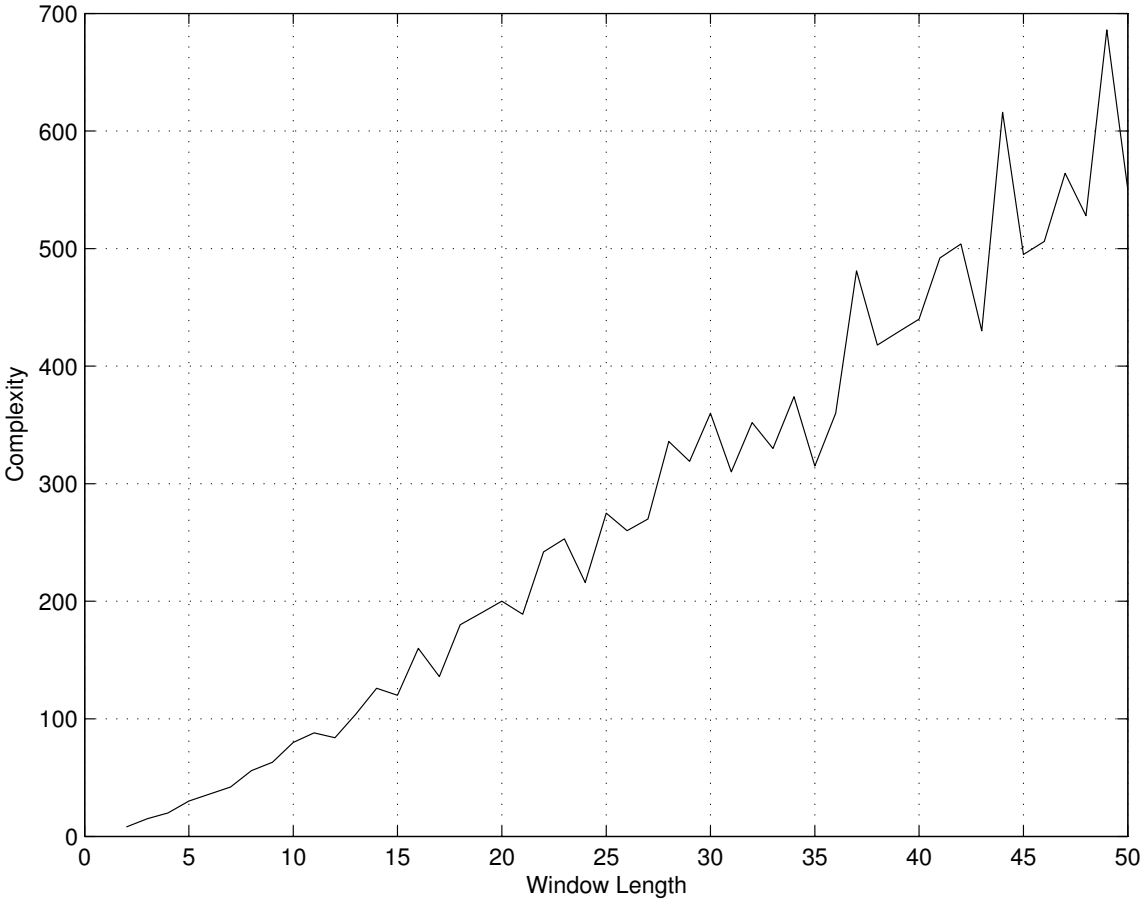

Fig. 7. The complexity of the first stage of the fast algorithm.

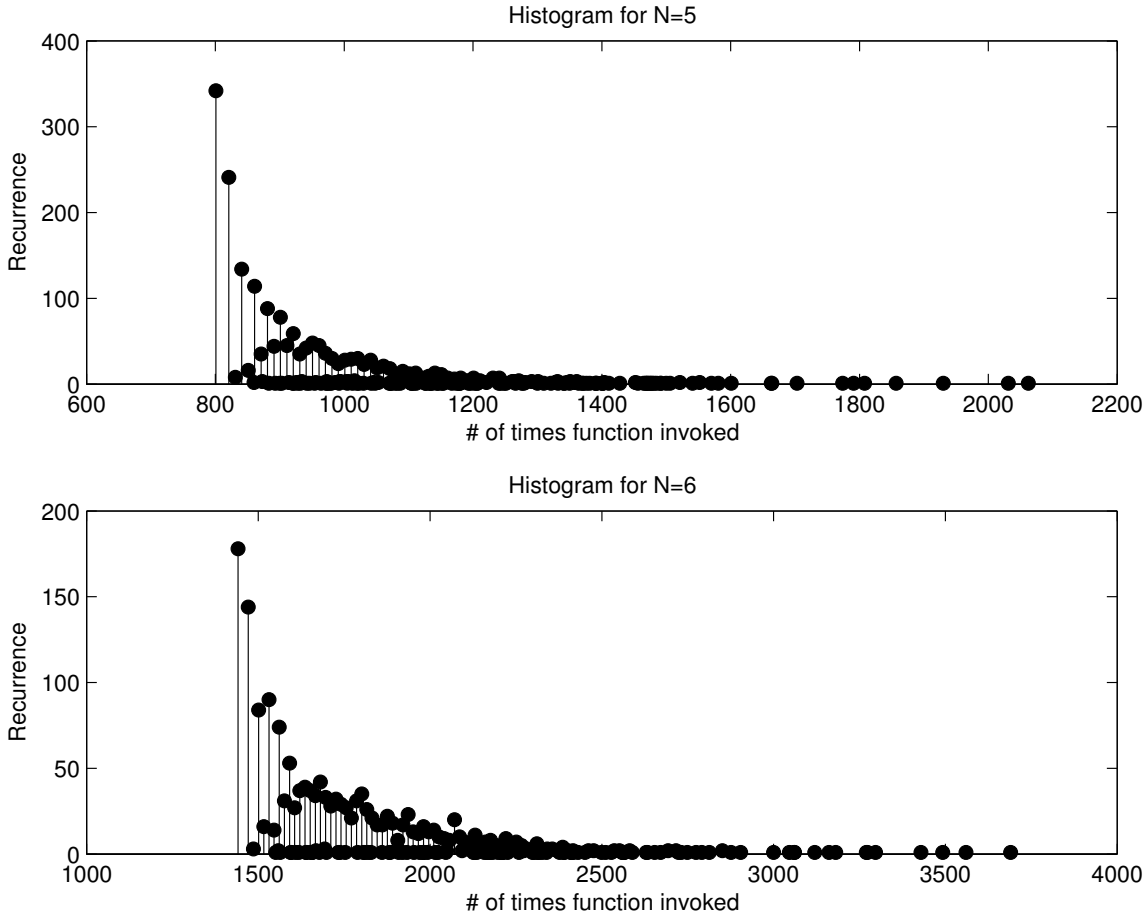

Fig. 8. The histograms for complexity of the last two stages combined for N=5 and 6.

A. Fast MS decoding of STDC

Before discussing the BER performance of the multi-symbol decoding of STDC, we take a look at the complexity of the fast algorithms devised above.

The first stage of the algorithm tries to find a solution that satisfies equation (2.30). A loop which fine tunes the values $\boldsymbol{G}_i$ for all $i = n, \ldots, n+1$ sequentially is executed several times. A simple measure of complexity for this stage can therefore be the number of times the loop is executed multiplied by the window length N. The

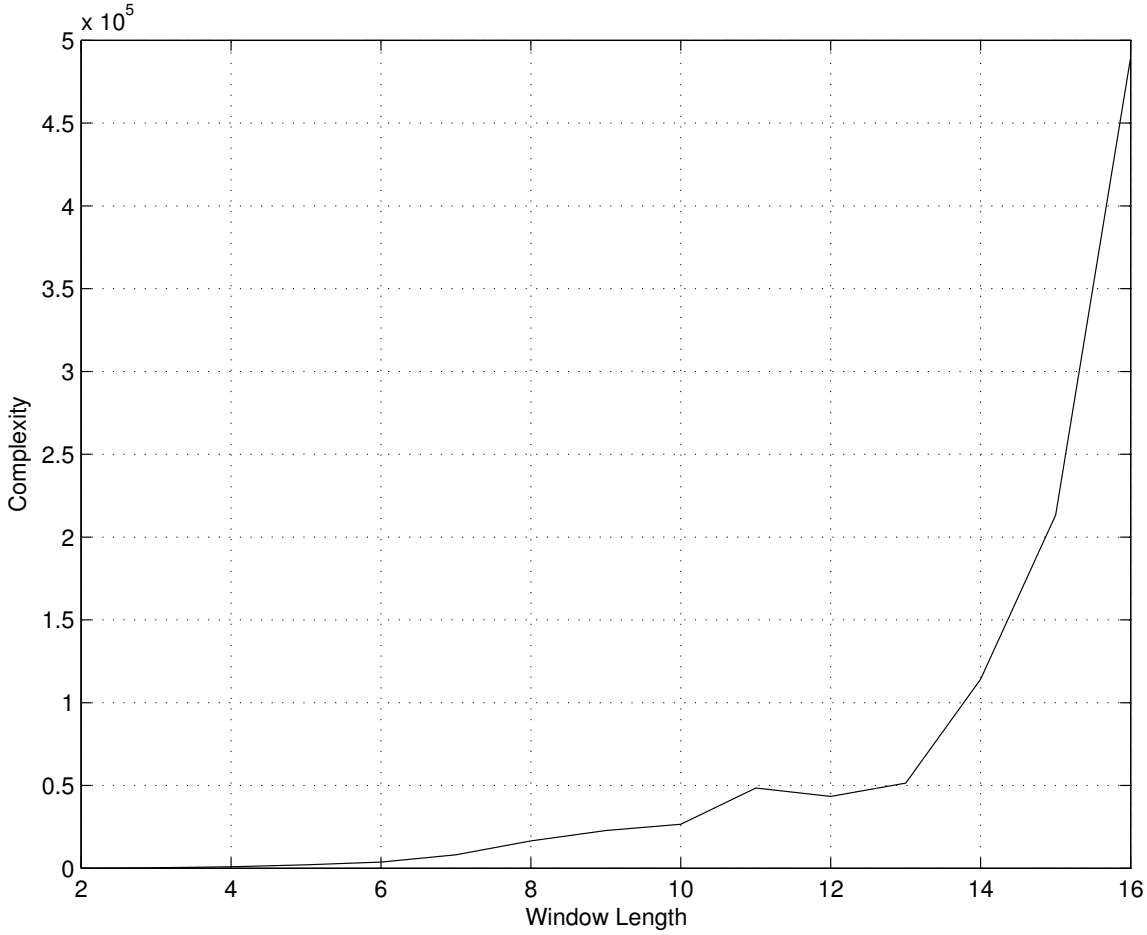

Fig. 9. The complexity of the last two stages combined of the fast algorithm.

complexity is statistically computed and is shown in Fig. 7. The complexity of this stage of the algorithm is found to be $\mathcal{O}(N)$ for higher values of N.

The basic constituent of the second and the third stage algorithms is the computation of the upper bound η_u. Each calculation comprises of smaller calculations for maximizing η_{ij}. We measure the joint complexity of the second and the third stage by counting the number of times the function for maximization of η_{ij} is called. To measure this we feed the system with a random input vector $\boldsymbol{y}_n$. For window

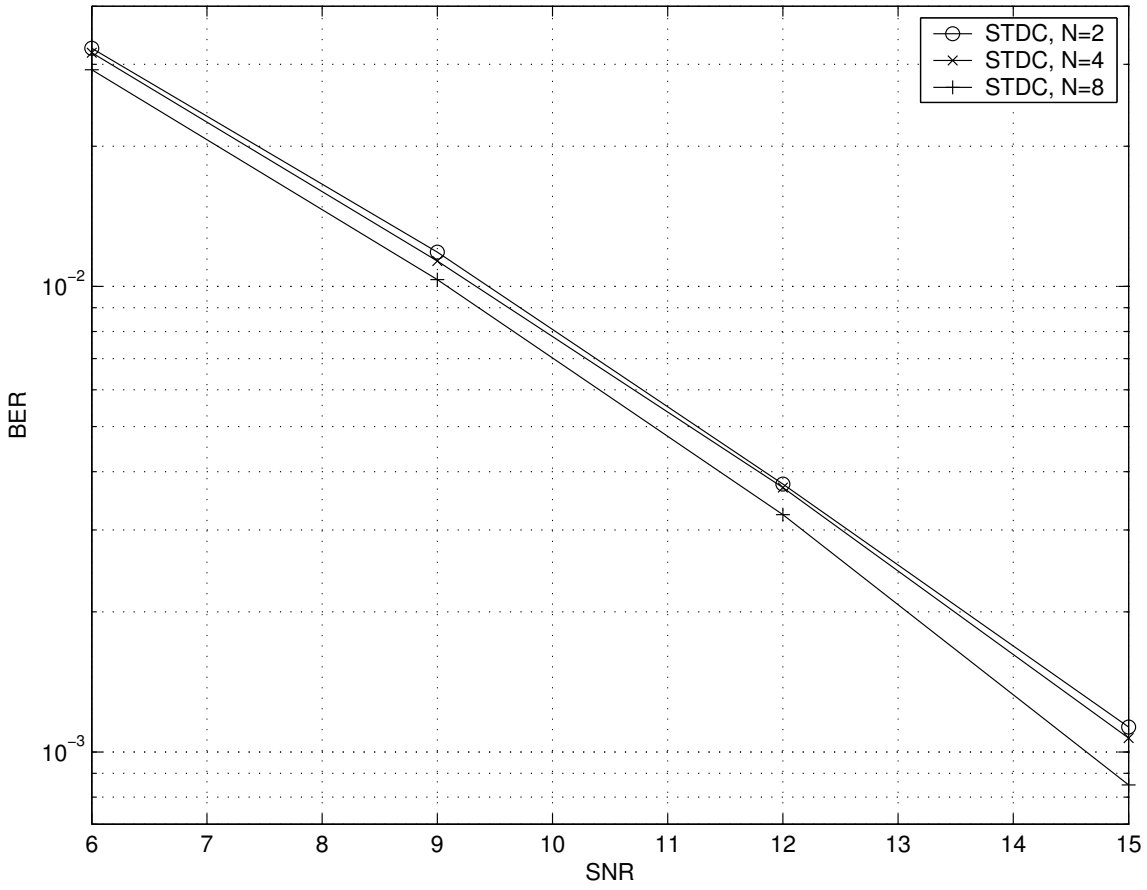

Fig. 10. The BER performance of the fast algorithm.

lengths $N = 5$ and 6, the histograms for the number of times the function for the maximization of η_{ij} is invoked are shown in fig. 8. The complexity of the algorithm is the worst case scenario, i.e., the case when the maximization function is invoked most number of times. The complexity of these stages is shown in fig. 9 and is found to be $\mathcal{O}(N^4)$. But as is evident from the shape of the histograms, most of the time the complexity is much less than the worst case scenario.

Fig. 10 shows the performance of MS-STDC. It is seen from the plots that the performance of the decoder is bettered with increasing window size. Fig. 11 shows

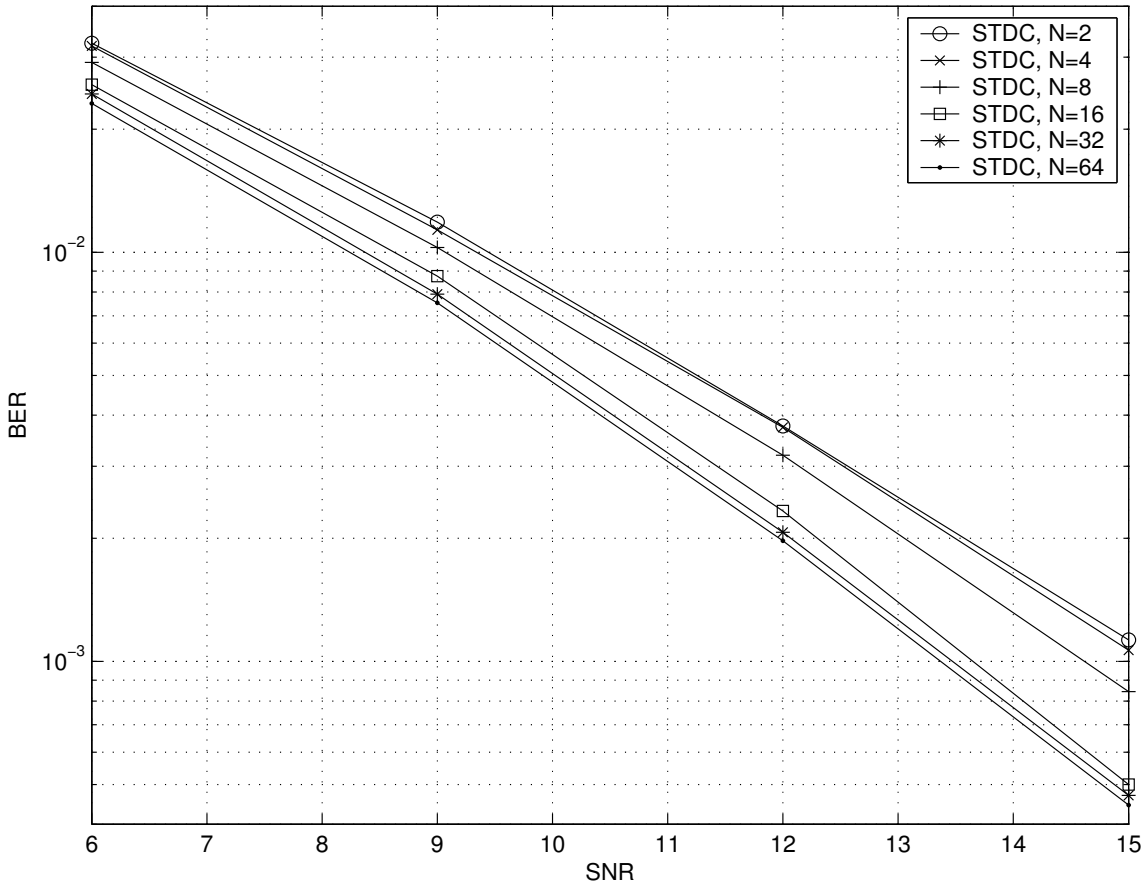

Fig. 11. The BER performance of the first stage of the fast algorithm.

the performance of the suboptimal estimate in the first stage of the algorithm. The performance closely matches that of the ML receiver. This algorithm can be used when the complexity and computing time is a big concern.

The performance of this receiver was also studied for fast-fading channels. Figs. 12 and 13 respectively show the performance plots of the ML receiver and the stage 1 receiver for a fading channel with a normalized Doppler frequency f_dT=0.01. It is seen from the simulation results that in a fading channel, increasing the window size infinitely does not result in better performance after a given window size. The

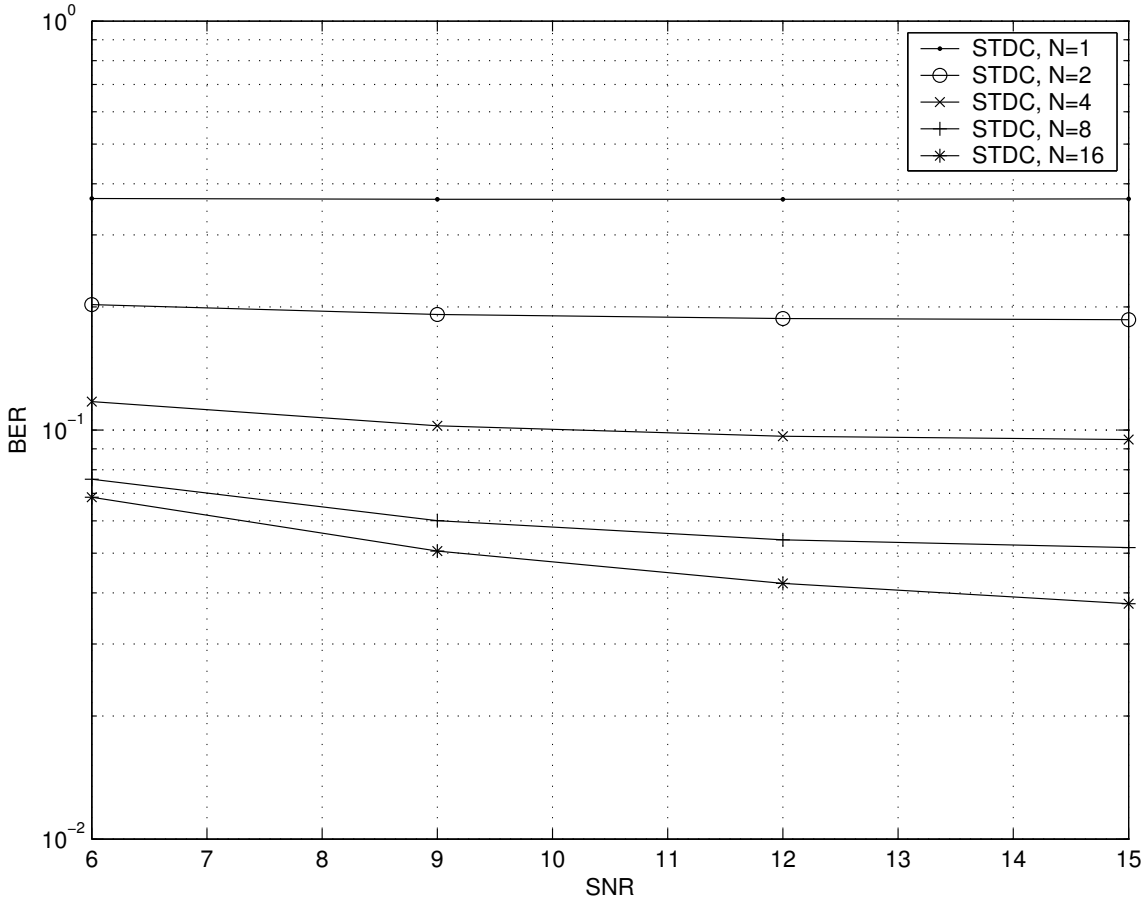

Fig. 12. The BER performance of the fast algorithm in a fading channel with a normalized Doppler frequency f_aT=0.01.

simulations show that the window size $N = 16$ gives the best results for low SNRs. Figs. 14 and 15 respectively show the performance plots of the ML receiver and the stage 1 receiver for a fading channel with a normalized Doppler frequency f_dT=0.001.

B. Iterative decoding of SPIHT + RCPC/CRC with STDC

Experiments are conducted with the 512×512 Lena image using the SPIHT + RCPC/CRC code. Again we assume fast fading channel with a normalized Doppler

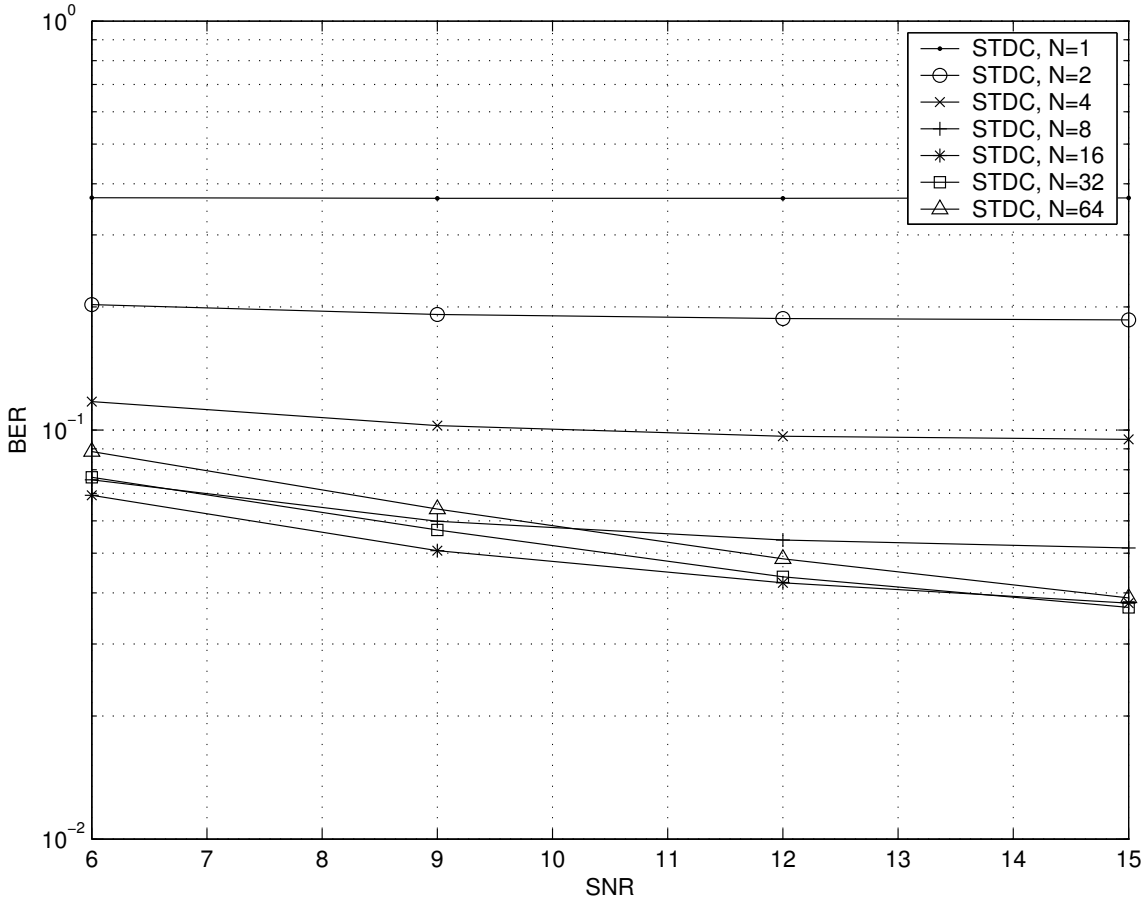

Fig. 13. The BER performance of the first stage of the fast algorithm in a fading channel with a normalized Doppler frequency f_aT=0.01.

$f_aT = 0.01$ and equal power between each transmit antenna and the receive antenna. The MAP decoding window length is 216; the transmission rate is fixed at 0.5 b/p with 8-PSK modulation. For a given number of turbo iterations (with four being the maximum), we use the criterion that out of 100 image transmissions, we will find the highest RCPC code rate that results in zero decoding error for the whole image in each transmission.

The SNR (E_b/N_0 in dB) vs. average MSE (converted to PSNR in dB) perfor-

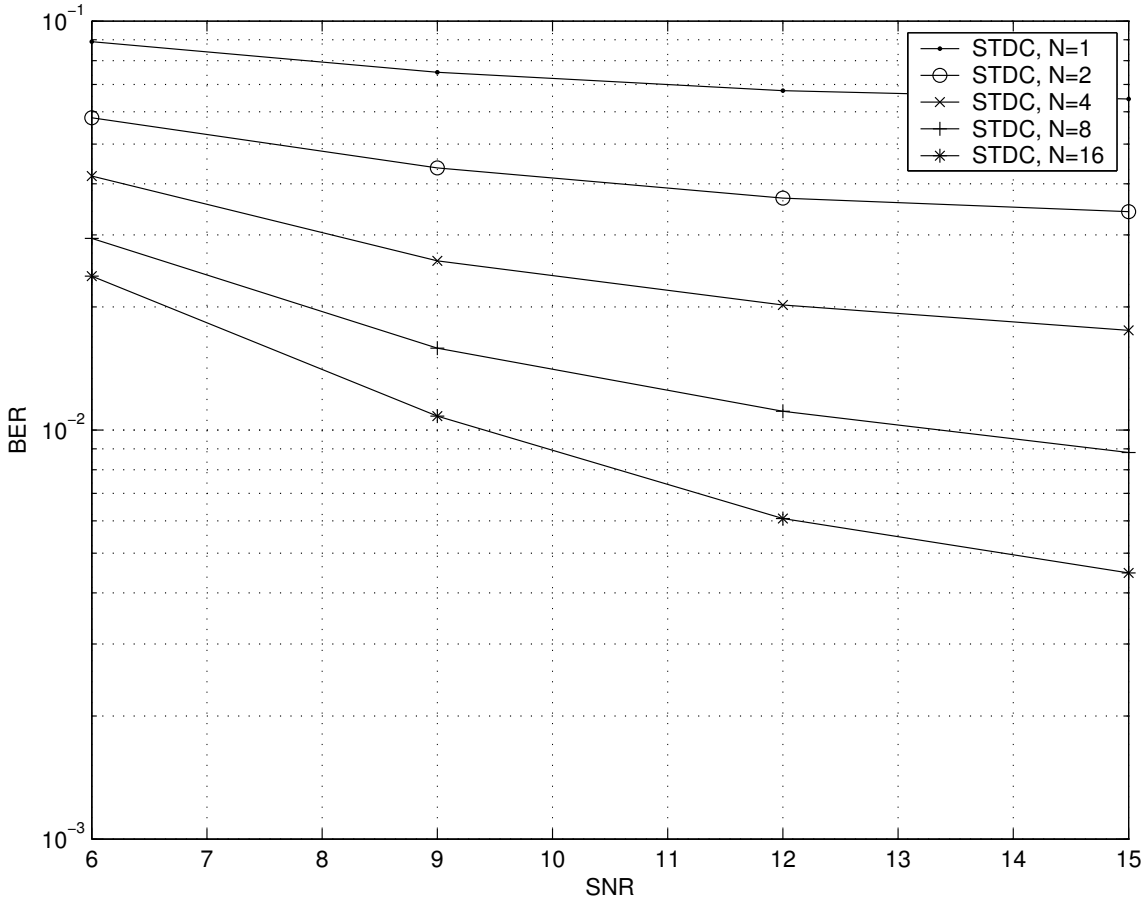

Fig. 14. The BER performance of the fast algorithm in a fading channel with a normalized Doppler frequency f_aT=0.001.

mance of our proposed system is depicted in Fig. 16. A gain of around 5 dB in PSNR is achieved with four iterations. The image qualities for varying PSNR's are given in figs. 17 and 18.

We have presented an iterative scheme for decoding differentially space-time coded MDs for image transmission over fading channels that performs well even without iterative decoding. We showed impressive performance gain (up to 5 dB in PSNR) with only four iterations.

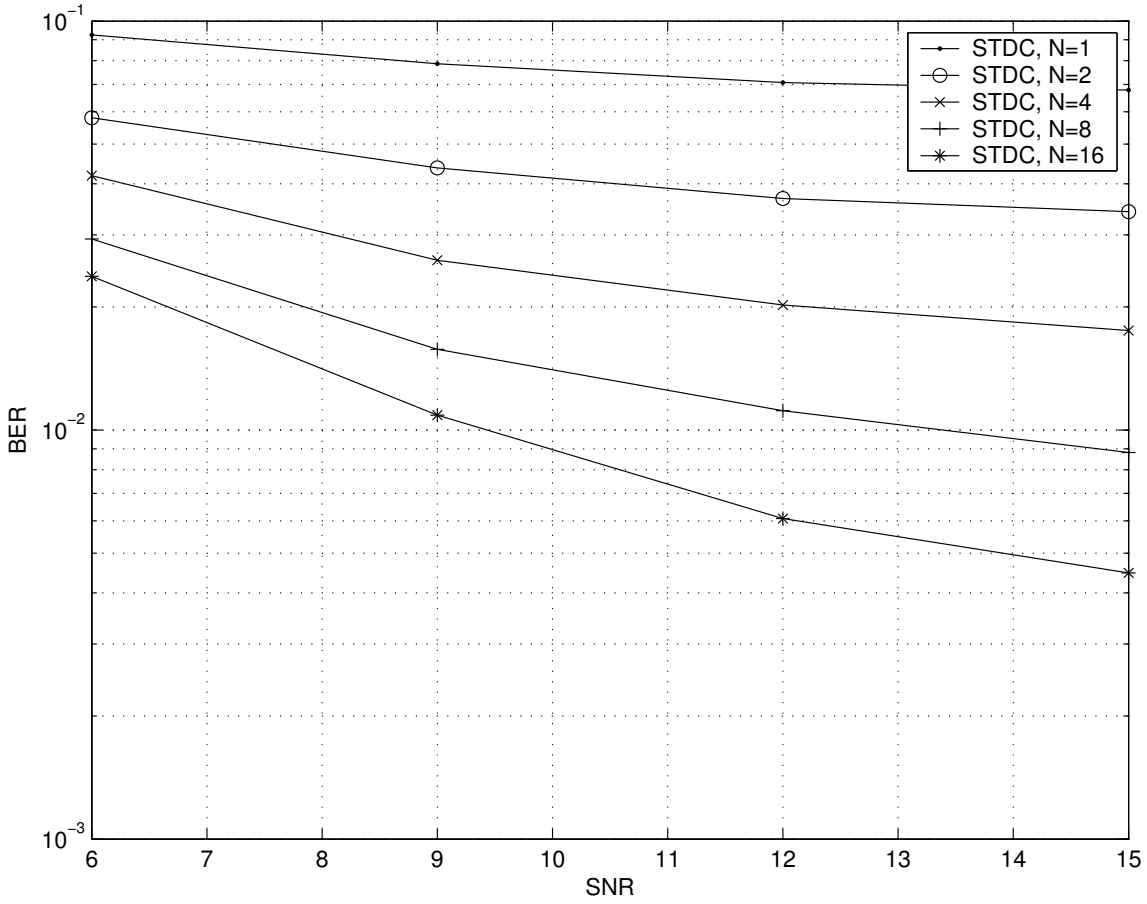

Fig. 15. The BER performance of the first stage of the fast algorithm in a fading channel with a normalized Doppler frequency f_aT=0.001.

C. Iterative decoding of SPIHT + RCPC/CRC with STC

Experiments are again conducted with the 512×512 Lena image using the SPIHT+ RCPC/CRC code. We assume fast fading channel with a normalized Doppler $f_aT = 0.01$ and equal power between each transmit antenna and the receive antenna. The window length is 216; the transmission rate is fixed at 0.5 b/p with QPSK modulation. For a given number of turbo iterations (with four being the maximum), we use the criterion that out of 100 image transmissions, we will find the highest RCPC code

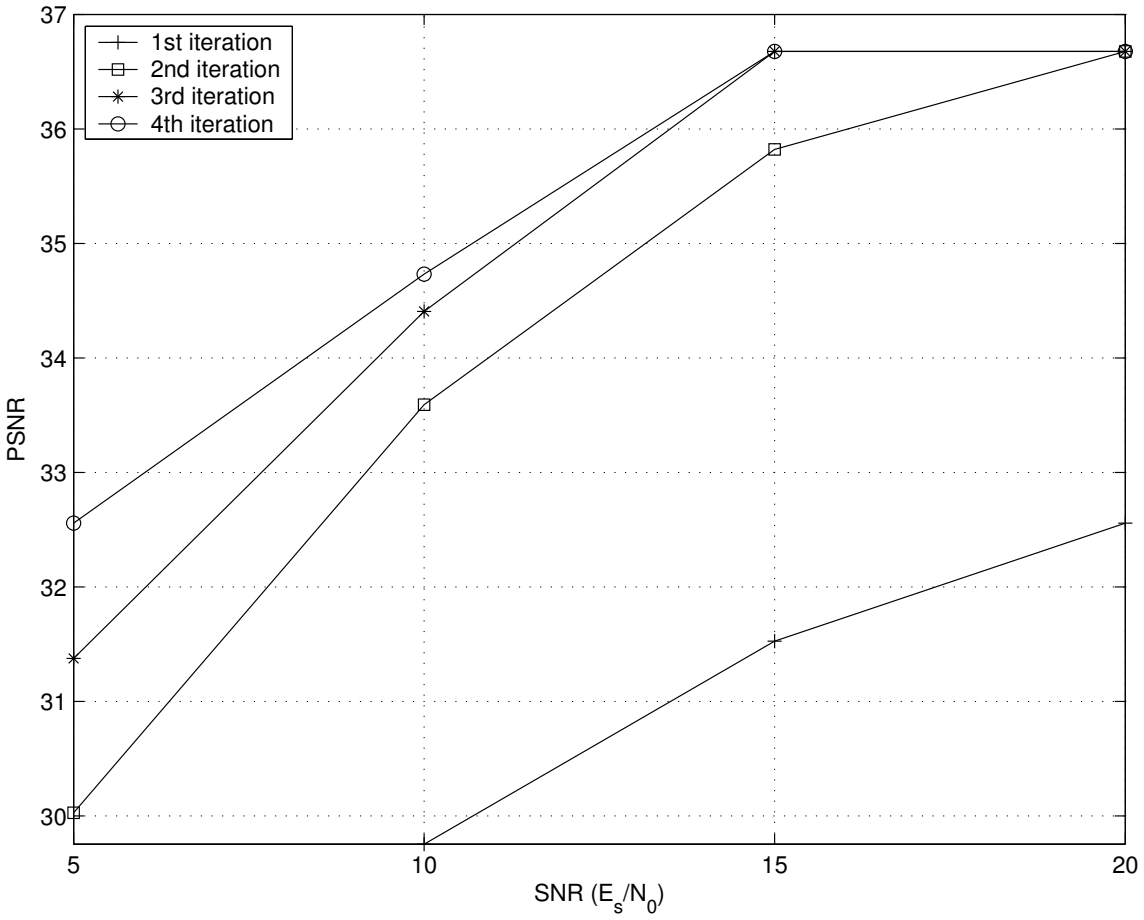

Fig. 16. The SNR (E_b/N_0 in dB) vs. average PSNR (in dB) performance of our proposed system.

rate that results in zero decoding errors. The SNR (E_b/N_0 in dB) vs. average MSE (converted to PSNR in dB) performance of our proposed system is depicted in Fig. 19. The perfect CSI at the receiver case is shown in dotted lines, while the linear predictor performance is shown in solid lines. A gain of around 7 dB in PSNR is achieved with four iterations. We see that the second iteration tends to eliminate more decoding errors than additional iterations. Also, the MAPEM approaches the perfect CSI performance after the third iteration.

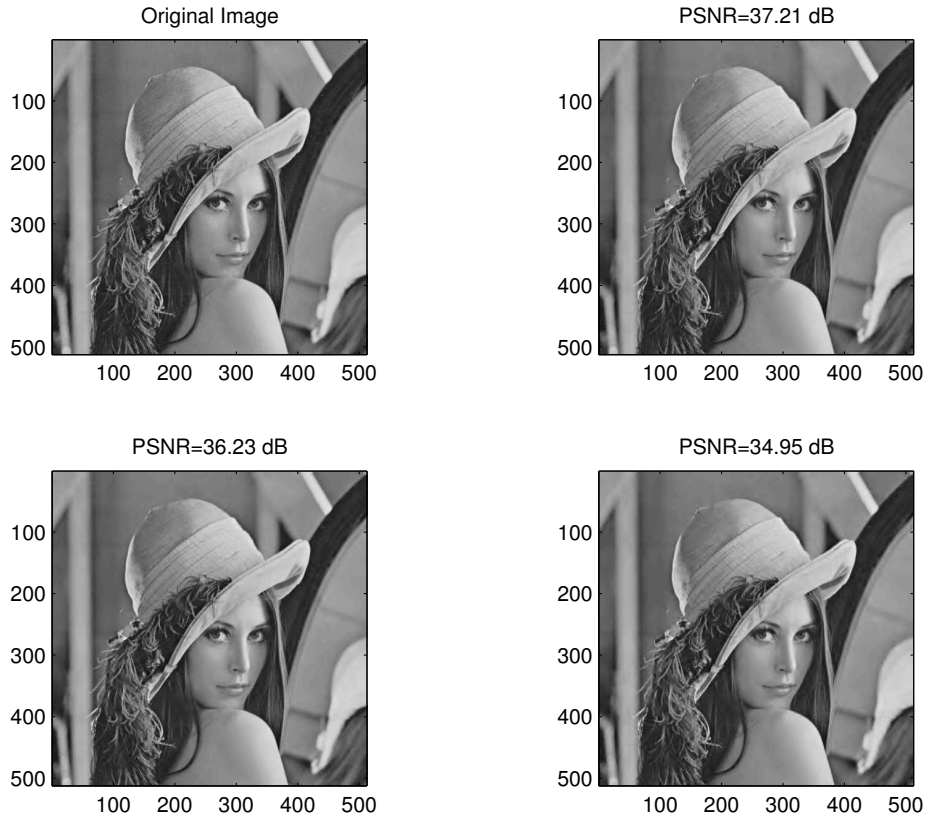

Fig. 17. The images with 37.21, 36.23 and 34.95 dB PSNR compared to the original image.

We have presented an iterative scheme for decoding STC-MD of images in fading channels that performs well even without iterative decoding. We showed impressive performance gain (up to 7 dB in PSNR) with only four iterations. Though this scheme requires a pilot symbol for channel estimation, the performance is better than the STDC-MDs.

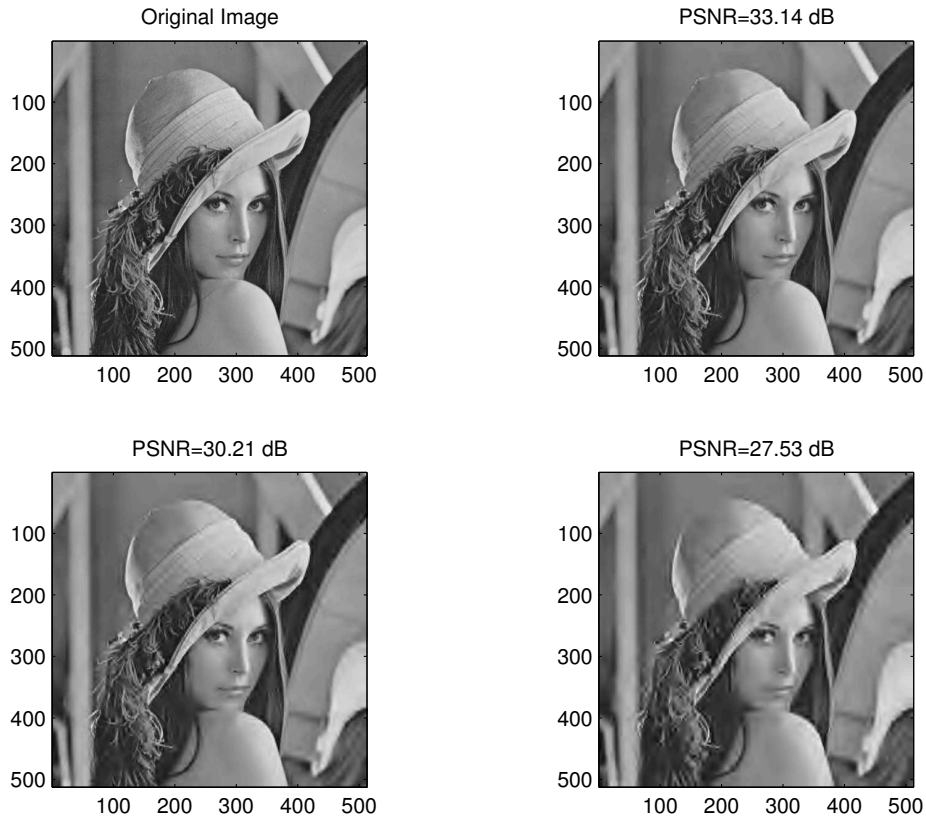

Fig. 18. The images with 33.14, 30.21 and 27.53 dB PSNR compared to the original image.

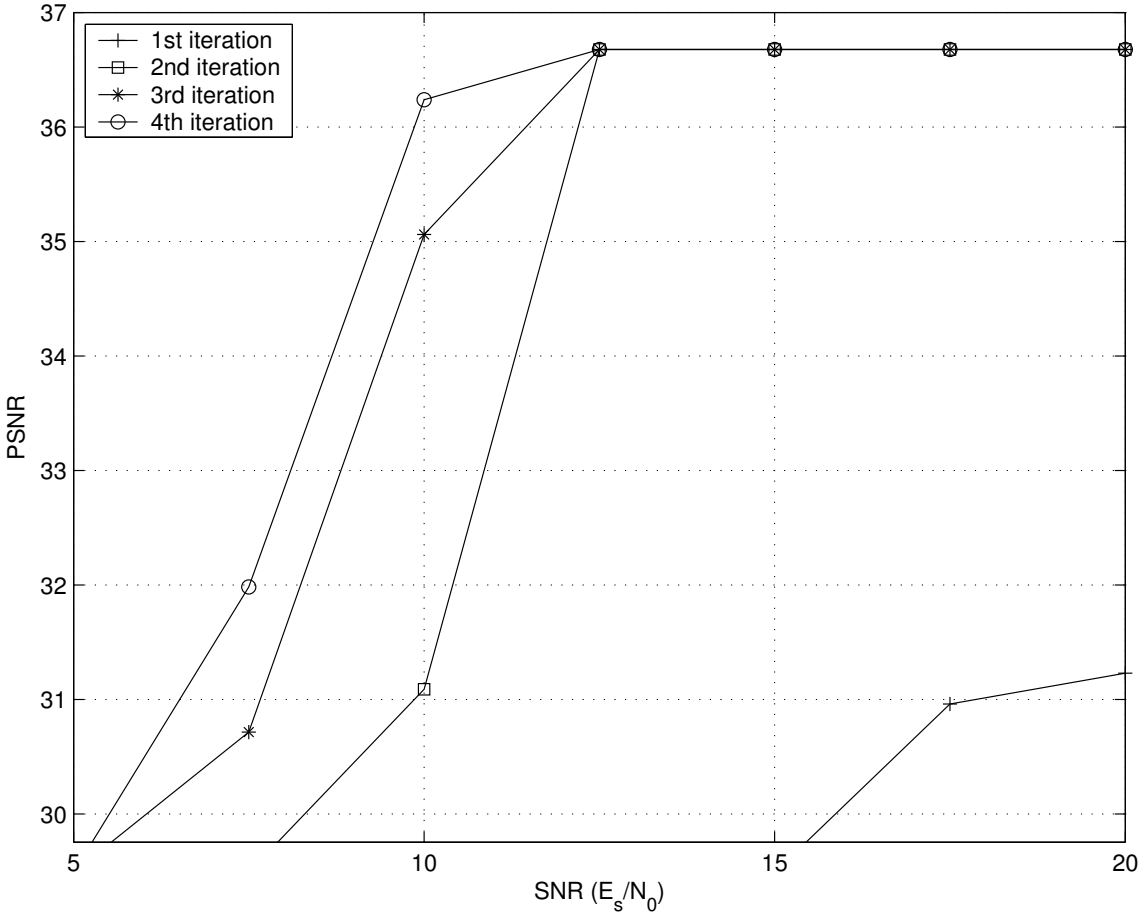

Fig. 19. The SNR (E_b/N_0 in dB) vs. average PSNR (in dB) performance of our proposed system.

REFERENCES

[1] S. Alamouti. "A simple transmit diversity technique for wireless communication," *IEEE Journal of Selected Areas in Communications*, vol. 16, no. 8, pp. 1451-1458, Oct., 1998.

[2] V.Tarokh and H. Jafarkhani. "A differential detection scheme for transmit diversity," *IEEE Journal on Selected Areas in Communications,* vol. 18, no. 7, pp. 1169-1174, July, 2000.

[3] B.L. Hughes. "Differential space-time modulation," *IEEE Transactions on Signal Processing*, vol. 46, no. 7, pp. 2567-2578, Nov., 2000.

[4] D. Divsalar and MK Simon. "Multiple-symbol differential detection of MPSK," *IEEE Transactions on Communications*, vol. 38, no. 3, pp. 300-308, Mar., 1990.

[5] P. Ho. and D. Fung. "Error performance of multiple symbol differential detection of PSK signals transmitted over correlated Rayleigh fading channels," *IEEE Transactions on Communications*, vol. 40, no. 10, pp. 1566-1569, Oct., 1992.

[6] K.M. Mackenthun, Jr. "A fast algorithm for multiple symbol differential detection of MPSK," *IEEE Transactions on Communications*, vol. 42, no. 234, pp. 1471-1474, Feb./Mar./Apr., 1994.

[7] Y.Liu and X.Wang. "Multiple-symbol decision-feedback differential space-time decoding in fading channels," *EURASIP Journal on Applied Signal Processing*, Special issue on Space-Time Coding and Its Applications, vol. 2002, no. 3, pp. 297-304, Mar., 2002.

[8] A. Nguyen and M. Ingram, "Iterative demodulation and decoding of differential space-time block codes," *in Proc. VTC'00*, vol. 5, pp. 2394-2400, Sept., 2000.

[9] L. Bahl, J. Cocke, F. Jelinek, and J. Raviv. "Optimal decoding of linear codes for minimizing symbol error rate," *IEEE Trans. Vehicular Tech.*, vol. 20, pp. 284-287, March 1974.

[10] V. Goyal, "Multiple description coding: compression meets the network," *IEEE Signal Processing Magazine*, vol. 18, pp. 74-93, September 2001.

[11] V. Vaishampayan, "Design of multiple description scalar quantizers," *IEEE Trans. Inform. Theory*, pp. 821-834, May 1993.

[12] Y. Wang, M. Orchard, V. Vaishampayan, and A. Riebman, "Multiple description coding using pairwise correlating transforms," *IEEE Trans. Image Processing*, pp. 351-366, March 2001.

[13] V. Goyal, J. Kovacevic, and M. Vetterli, "Multiple description transform coding: robustness to erasures using tight frame expansions," *in Proc. ISIT*, Cambridge, MA, August 1998, pp. 408.

[14] R. Puri and K. Ramchandran, "Multiple description source coding through forward error correction codes," *in Proc. 33rd Asilomar Conference on Signals, Systems, and Computers*, Pacific Grove, CA, October 1999, pp. 342-346.

[15] A. Mohr, E. Riskin, and R. Ladner, "Generalized multiple description coding through unequal loss protection," *in Proc. ICIP'99*, Kobe, Japan, October 1999, pp. 411-415.

[16] C. Berrou and A. Glavieux, "Near optimum error correcting coding and decoding: turbo-codes," *IEEE Transactions on Communications*, vol. 44, pp. 1261-1271, October 1996.

[17] K. Narayanan and G. Stuber, "A serial concatenation approach to iterative demodulation and decoding," *IEEE Transactions on Communications*, vol. 47, pp. 956-961, July 1999.

[18] M. Srinivasan, "Iterative decoding of multiple descriptions," *in Proc. DCC'99*, Snowbird, UT, March 1999, pp. 463-472.

[19] P. G. Sherwood and K. Zeger, "Progressive image coding for noisy channels," *IEEE Signal Processing Letters*, vol. 4, pp. 189-191, July 1997.

[20] J. Hagenauer, "Rate-compatible punctured convolution codes (RCPC codes) and their applications," *IEEE Transactions on Communications*, vol. 36, pp. 389-400, 1988.

[21] G. Foschini, "Layered space-time architecture for wireless communication in a fading environment when using multiple antennas," *Bell Labs Tech. Journal*, vol. 1, pp. 41-59, 1996.

[22] Ben Lu, X. Wang and Ye Li, " Iterative receivers for space-time block-coded OFDM systems in dispersive fading channels," *IEEE Trans. Wireless Communications*, vol. 1, pp. 213-225, April 2002.

[23] C.N. Georghiades and J.C. Han, " Sequence estimation in the presence of random parameters via the EM algorithm, " *IEEE Transactions on Communications*, vol. 45, pp. 300-308, March 1997.

[24] W. Jakes, *Microwave Mobile Communications*, New York: Wiley, 1974.

[25] R. Raheli, A. Polydoros and C. Tzou. "Per-survivor processing: a general approach to MLSE in uncertain environments," *IEEE Transactions on Communications*, vol. 43, pp. 354-364, 1995.

[26] R. Hamzaoui, V. Stankovic, and Z. Xiong, "Rate-based versus distortion-based optimal joint source-channel coding," *in Proc. DCC'02*, Snowbird, UT, April 2002, pp. 63-72.

[27] V. Tarokh, N. Seshadri, and R. Calderbank, "Space-time codes for high data rate wireless communication: performance criterion and code construction," *IEEE Trans. Inform. Theory*, vol. 44, pp. 744-765, March 1998.

VITA

Rohit Singhal was born in Jaipur, India in September, 1977. He received his baccalaureate degree in electronics and electrical communication engineering, with honors, from the Indian Institute of Technology, Kharagpur, India in July, 2000.

He can be reached at the Department of Electrical Engineering, Texas A&M University, College Station, TX 77843.

This document was typeset in LaTeX by Rohit Singhal.